Precambrian Research 242 (2014) 82–95

Contents lists available at ScienceDirect

Precambrian Research

journal homepage: www.elsevier.com/locate/precamres

3.45 Ga granitic gneisses from the Yangtze Craton, South China: Implications for Early Archean crustal growth

Jing-Liang Guo, Shan Gao*, Yuan-Bao Wu, Ming Li, Kang Chen, Zhao-Chu Hu, Zheng-Wei Liang, Yong-Sheng Liu, Lian Zhou, Ke-Qing Zong, Wen Zhang, Hai-Hong Chen

State Key Laboratory of Geological Processes and Mineral Resources, China University of Geosciences, 430074 Wuhan, China

ARTICLE INFO

Article history:
Received 26 March 2013
Received in revised form
23 December 2013
Accepted 30 December 2013
Available online 6 January 2014

Keywords:
Paleoarchean
Crustal growth
Granitic gneiss
Zircon
Yangtze Craton
South China

ABSTRACT

Zircon U–Pb–Lu–Hf–O isotopic compositions of two granitic gneisses from the Kongling Terrain in the Yangtze Craton, South China were determined by SIMS, LA-ICP-MS and LA-MC-ICP-MS. Whole rocks of the two samples were analyzed for major and trace element compositions. The SIMS and LA-ICP-MS data reveal similar five zircon age groups of 3.4, 3.3, 2.9, 2.7, and 2.0 Ga for both gneisses. Three groups (magmatic Group A, metamorphic Group B, and overgrowth Group C) of the 3.4 Ga zircons were identified based on their CL images. These three groups have indistinguishable ages and Th/U ratios. Groups A and B show identical $^{176}Hf/^{177}Hf$ (*t*), although Group C was too thin to be analyzed by LA-ICP-MS. Taken together, zircons from the two samples with 98–102% age concordance give weighted average SIMS ages of 3434.3 ± 9.6 Ma (2σ, MSWD = 13, n = 8) for Group A, 3446.0 ± 8.8 Ma (2σ, MSWD = 10.7, n = 15) for Group B, and 3479 ± 26 Ma (2σ, MSWD = 0.49, n = 2) for Group C. Groups A and B together yield an upper intercept age of 3457 ± 14 Ma (2σ, MSWD = 0.85, n = 23). The LA-ICP-MS data yield weighted average ages of 3442 ± 19 Ma (2σ, MSWD = 0.17, n = 7) for Group A and 3435 ± 11 Ma (2σ, MSWD = 0.44, n = 16) for Group B. They yield an upper intercept age of 3443 ± 13 Ma (2σ, MSWD = 0.63, n = 23). These SIMS and LA-ICP-MS ages are consistent. We propose that the above SIMS and LA-ICP-MS ages of Groups A and B are the best estimates of the granitic magmatism and the subsequent metamorphism. The metamorphism must have occurred after the granitic magmatism within a few tens of million years, as constrained by their age errors. Accordingly, these two granitic gneisses represent the oldest rocks currently known in South China. They predate the previously reported 3300-Ma-old trondhjemitic gneiss from the Kongling Terrain by 150 Ma.

The 3.4 Ga zircons show near chondritic ε_{Hf} (*t*) (−0.7 ± 1.0, 2σ, MSWD = 1.14, n = 8), which is below the coeval value of the depleted mantle. This suggests that the granitic magma contained materials of pre-existing continental crust. Their higher-than-mantle $\delta^{18}O$ values (6.1–6.4‰) imply that such materials must have been interacted with surface water. Crust formation ages (T_{DM2}) of the 3.4 Ga zircons vary from 3.9 to 3.6 Ga with a weighted average of 3703 ± 27 Ma (2σ, MSWD = 1.05, n = 7). Our results support previous studies that the Yangtze Craton may have contained the continental crust as old as 3.8 Ga.

Among the younger age groups, the 3.3 Ga zircons exhibit $^{176}Hf/^{177}Hf$ (*t*) and $\delta^{18}O$ values similar to the 3.4 Ga zircons, suggesting that they were altered from the 3.4 Ga zircons. The 2.9 and 2.7 Ga zircons in both samples are rare and magmatic. Their $^{176}Hf/^{177}Hf$ (*t*) ratios are distinct from the 3.4 Ga zircons, indicating different sources. These two age groups are consistent with the 2.9 Ga trondhjemitic–tonalitic–granodioritic and the 2.7 Ga A-type granitic magmatism in the Kongling Terrain. The 2.0 Ga metamorphic zircons, regardless of being concordant or discordant, have $^{176}Hf/^{177}Hf$ (*t*) ratios overlapping those of the 2.7 Ga zircons, suggesting a common source. In contrast, $\delta^{18}O$ of the 2.0 Ga zircons is strongly variable and positively correlated with age concordance. The low $\delta^{18}O$ (down to 3.1‰) requires interaction with hydrothermal fluid. These results suggest that at least some of the 2.0 Ga zircons were likely to have been altered from the 2.7 Ga zircons by hydrothermal fluid.

1. Introduction

The first two billion years of the Earth's history are the most important period during which the majority of the continental crust was generated (e.g. Armstrong and Harmon, 1981; Taylor and

* Corresponding author. Tel.: +86 027 6788 3040; fax: +86 027 6788 5096.
E-mail address: sgao@263.net (S. Gao).

0301-9268/$ – see front matter © 2014 Elsevier B.V. All rights reserved.
http://dx.doi.org/10.1016/j.precamres.2013.12.018

McLennan, 1985; Hawkesworth et al., 2010; Cawood et al., 2012). Crustal rocks formed during this period provide direct information on the early differentiation and evolution of the shallow Earth. These ancient rocks, however, are difficult to preserve. >3.8 Ga rocks only occur in the Acasta Gneiss Complex in Northwest Territories of Canada (Bowring and Williams, 1999), the Itsaq Gneiss Complex in West Greenland (Nutman et al., 1996), and the Anshan area in the northeastern North China Craton (Liu et al., 1992). Paleoarchean (>3.2 Ga) rocks, although covering a relatively wider area, are still very rare when compared with the total area of the continental crust (Condie, 2007). Such ancient rocks commonly experienced multi-stage of subsequent alteration processes (e.g., deformation, metamorphism and/or migmatization), which strongly blurred or even eliminated the primary chemical and isotopic compositions of the whole rocks.

Zircon, as a common U–Th-bearing accessory mineral, has shown its superiority in resistance to later modifications. Integration of zircon U–Pb–Lu–Hf–O isotopic compositions constrains the age and nature of magmatic and metamorphic events (e.g., Hawkesworth and Kemp, 2006; Zheng et al., 2006b; Harrison et al., 2008; Li et al., 2010a, 2012; Bell et al., 2011; Hiess et al., 2011).

In China, the oldest rocks appear to be 3.8 Ga trondhjemitic–tonalitic–granodioritic (TTG) gneisses from the Anshan area (Liu et al., 1992), 3.66 Ga felsic granulite xenoliths from the Xinyang area (Zheng et al., 2004) in the North China Craton, and 3.3 Ga TTG gneisses (Gao et al., 2011) and 3.2 Ga migmatites (Jiao et al., 2009) from the Kongling Terrain in the Yangtze Craton, South China. In the Yangtze Craton, existence of the continental crust older than 3.8 Ga was suggested by Hf model ages of the Paleoarchean zircons in 3.3–3.2 Ga orthogneisses and migmatites (Jiao et al., 2009; Gao et al., 2011). Nevertheless, the Early Archean history (3.8–3.3 Ga) of the Yangtze Craton is poorly known.

In this paper, we report zircon U–Pb–Lu–Hf–O isotopic and whole-rock major and trace element compositions of two granitic gneisses from the northeastern Kongling Terrain, Yangtze Craton. Our results indicate that these two orthogneisses were formed at 3.45 Ga. They represent the oldest rocks currently known in South China.

2. Geological background

South China consists of the Yangtze Craton in the northwest and the Cathaysia Block in the southeast (Fig. 1a). These two blocks were amalgamated during the Neoproterozoic (Li et al., 2009a). The Kongling Terrain is located in the northeastern Yangtze Craton. It has an oval dome structure, covering an area of ~360 km^2 (Fig. 1b). It is divided into two segments: the North and the South Kongling Terrains. The North Kongling Terrain is dominated by Archean TTG-granitic gneisses and metasedimentary rocks (Fig. 1c) (Gao et al., 1999, 2011). Contrastively, the South Kongling Terrain is dominated by Neoproterozoic TTG intrusions (the Huangling Batholith) (Ling et al., 2006; Zhang et al., 2008). They emplaced into Archean TTG and metasedimentary rocks that are equivalents to those Archean rocks in the North Kongling Terrain (Gao et al., 2011) (Fig. 1b).

Previous studies revealed three major Archean crustal-growth episodes in the Kongling Terrain: 3.3–3.2 Ga, 2.9–2.8 Ga, and 2.7–2.6 Ga (Gao et al., 1999, 2011; Qiu et al., 2000; Zhang et al.,

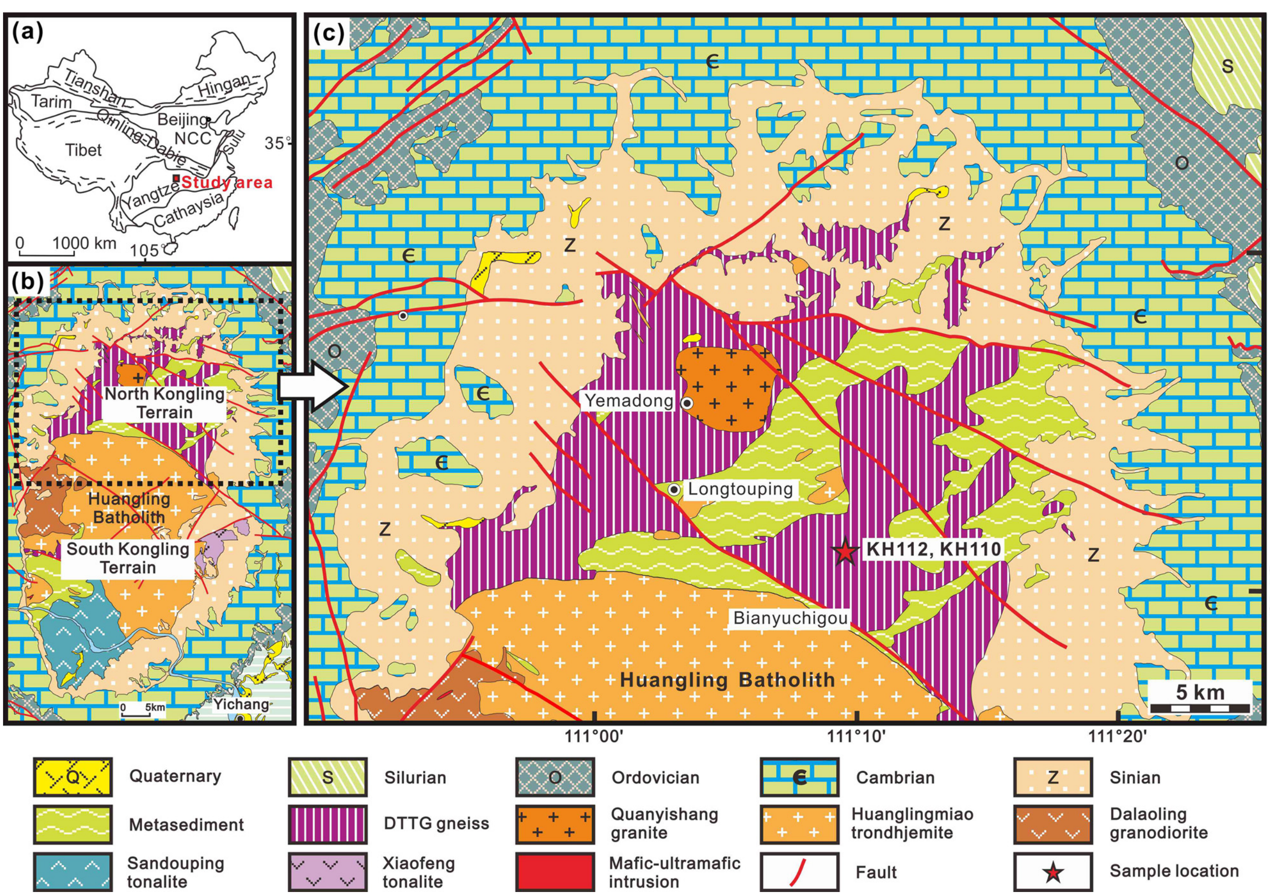

Fig. 1. Geological map of the Archean Kongling Terrain (modified from Gao et al., 2011). (a) Major tectonic divisions of China. NCC denotes the North China Craton. (b) Structure and division of the Kongling Terrain. (c) Geological map of the North Kongling Terrain. Star denotes the sample location for granitic gneisses KH112 and KH110 in this study. DTTG = dioritic–trondhjemitic–tonalitic–granodioritic.

2006a; Jiao et al., 2009; Chen et al., 2013). The 3.3–3.2 Ga TTG gneisses and migmatites were locally preserved in the widespread 2.9–2.8 Ga TTG rocks (Gao et al., 1999, 2011; Zhang et al., 2006a; Jiao et al., 2009). The 2.7–2.6 Ga A-type granitic gneisses were recently discovered in the eastern North Kongling Terrain, which marks the termination of subduction-related TTG magmatism with significant juvenile crustal additions (Chen et al., 2013). Crustal materials as old as 3.8 Ga have only been inferred from zircon Hf model ages (Jiao et al., 2009; Gao et al., 2011). Although one 3.8 Ga detrital zircon from a Neoproterozoic sandstone was reported in the Kongling Terrain (Zhang et al., 2006c), its source was largely uncertain.

3. Sample descriptions

Two fresh granitic gneisses KH112 and KH110 were taken from Bianyuchigou in the North Kongling Terrain (31°09′30″ N, 111°09′40″ E) (Fig. 1c). The region is covered by vegetation. The exposed lithology is mainly gray gneiss, which is strongly foliated and locally migmatized with quartzo-feldspathic bands and thin biotite-rich interlayers. They were cut by plagiogranitic or quartz veins.

KH112 has a mineral assemblage of ~40% quartz, ~40% plagioclase, ~15% orthoclase, and ~5% biotite in volume. It consists of quartzo-feldspathic bands (5–10 cm thick) and biotite-rich interlayers (1–2 cm thick). Plagiogranitic pods exist in the quartzo-feldspathic bands, and the adjoining biotite-rich layer is bended. Feldspar is partially weathered (Fig. 2a and b). Minor biotite in the quartzo-feldspathic bands shows no orientation (Fig. 2a), while biotite from the biotite-rich layers is elongated, deformed, and oriented (Fig. 2b).

KH110 is similar to KH112. It has a mineral assemblage of ~40% quartz, ~30% plagioclase, ~20% orthoclase and ~10% biotite in volume. Quartzo-feldspathic bands are usually 2–5 cm thick and are nearly free of biotite (Fig. 2c). The biotite-rich layers are generally thinner than 0.5 cm and consist of euhedral biotite and fine-grained feldspar (Fig. 2d). Plagiogranitic pods also exist. Coarse-grained feldspar adjacent to the biotite-rich layers was partially recrystallized into fine grains and shows a myrmekitic texture (Fig. 2d).

4. Analytical methods

4.1. Whole-rock analysis

Rock samples were crushed and then powdered in an agate mill down to <200 mesh. Major oxides were analyzed by XRF (Rikagu RIX 2100) using fused glass disks at the State Key Laboratory of Continental Dynamics, Northwest University, Xi'an, China. Analyses of USGS basalt and andesite standards (BCR-2, BHVO-1 and AGV-1) indicate precision and accuracy better than 5% for major elements (Rudnick et al., 2004). Trace elements were analyzed by Agilent 7500a ICP-MS with shielded torch at the State Key Laboratory of Geological Processes and Mineral Resources, China University of Geosciences, Wuhan. Sample powders were digested by acid in Teflon bombs under high pressure (7–9 MPa). Detailed sample-digestion procedure for ICP-MS analysis was reported by Liu et al. (2008b). For most trace elements, our measured values of BCR-2, BHVO-1 and AGV-1 agree with their recommended values from GeoReM (http://georem.mpch-mainz.gwdg.de/) within 5% difference.

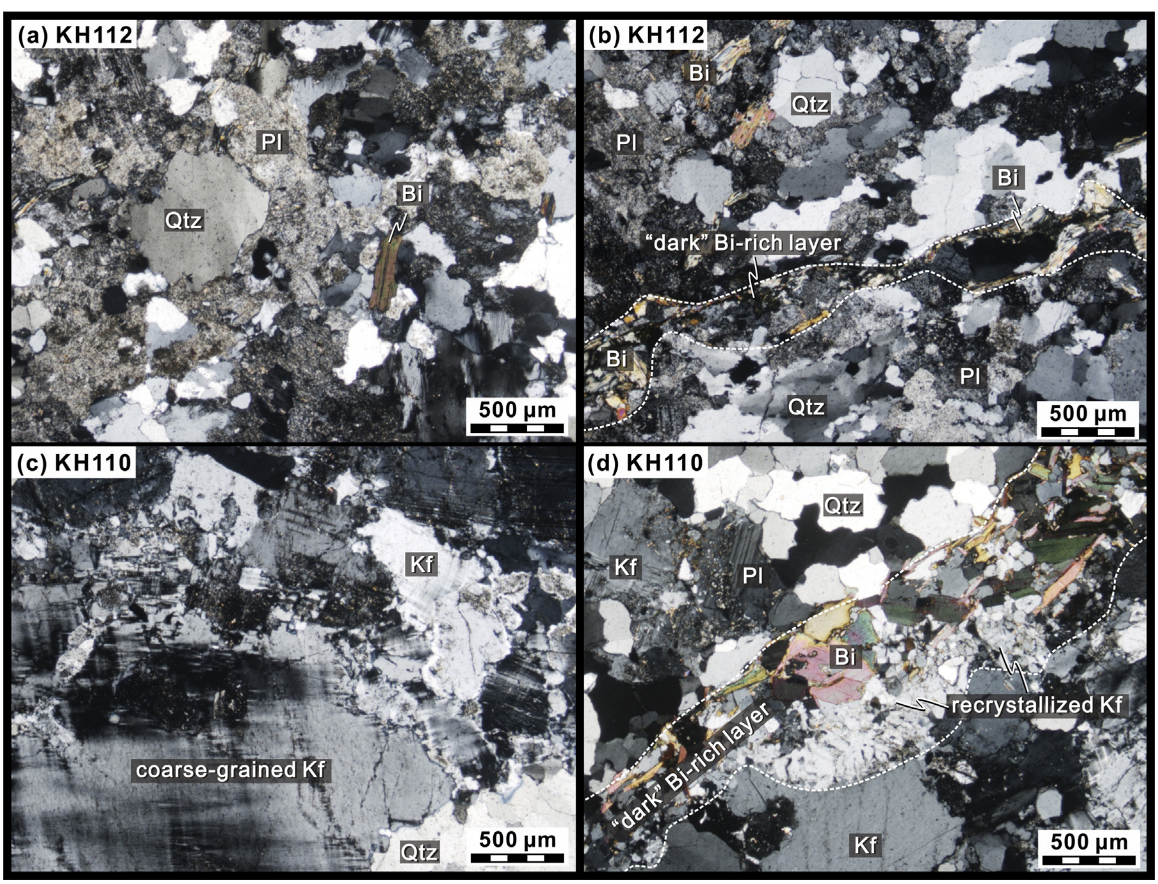

Fig. 2. Micrographs under cross-polarized lights for granitic gneisses KH112 (a and b) and KH110 (c and d). (a) A medium- to coarse-grained domain. (b) A less than 0.5-mm-thick fine-grained biotite-rich layer is marked out by two white dashed lines. The cloudy mineral is weathered feldspar. (c) A coarse-grained biotite-free domain. The size of K-feldspar is up to 2 mm. (d) White dashed lines indicate boundaries of a 1-mm-thick biotite-rich layer. Bi = biotite; Pl = plagioclase; Kf = K-feldspar; Qtz = quartz.

4.2. Zircon analysis

More than 10 mg of zircon was separated by conventional magnetic and heavy liquid methods for each sample. According to color, size, shape, and transparence under a binocular microscope, the zircons were selected and mounted along with fragments of zircon standards including 91500 (Wiedenbeck et al., 1995), GJ-1 (Jackson et al., 2004), Penglai (Li et al., 2010b), Qinghu (Li et al., 2009b) and Plešovice (Sláma et al., 2008) on a double-sided adhesive tape, and then casted in epoxy resin in a 1-in.-diameter mount. The mount was polished to expose the center of the zircon grains. All zircons were documented with optical photomicrographs under both transmitted and reflected lights in order to avoid inclusions and cracks in later U–Pb, Lu–Hf and O analysis. Dilute HNO_3 and pure ethanol were used to clean the surface of the grain mounts before analysis in order to avoid Pb contamination.

4.2.1. CL imaging

CL images were used to reveal the internal structures of zircons and to help select optimum spot locations for later in situ analysis. The imaging was done at the State Key Laboratory of Continental Dynamics, Xi'an and the State Key Laboratory of Geological Processes and Mineral Resources, Wuhan. The laboratory in Xi'an uses a FEI Quanta 400 FEG high resolution emission field environmental scanning electron microscope connected to an Oxford INCA350 energy dispersive system (EDS) and a Gatan Mono CL3+ system. The working distance for the CL system was 8.4 mm, while the EDS used a spot size of 6.7 nm with a voltage of 10 kV. The Wuhan laboratory operates a FEI Quanta 450 FEG scanning electron microscope coupled with a Gatan Mono CL4+ system. A spot size of 5 nm and a working distance of 13.8–15 mm were used.

4.2.2. SIMS O isotope analysis

As minimal sample amount is required, the oxygen isotope analysis was carried out prior to U–Pb dating and Hf isotope analysis. The analysis used a Cameca IMS 1280 ion microprobe at the Institute of Geology and Geophysics, Chinese Academy of Sciences, Beijing. Analytical procedures were similar to those described by Li et al. (2010b). The spot size was about 20 μm in diameter. The Cs^+ primary ion beam was accelerated at 10 kV, with an intensity of 2 nA (Gaussian mode with a primary beam aperture of 200 μm to reduce aberrations), and rastered over a 10 μm distance. Oxygen isotopes were measured using multi-collection mode on two off-axis Faraday cups. Measured $^{18}O/^{16}O$ ratios were normalized to the Vienna Standard Mean Ocean Water (VSMOW, $^{18}O/^{16}O = 0.0020052$), referred as $\delta^{18}O = [(^{18}O/^{16}O)_{sample}/(^{18}O/^{16}O)_{VSMOW} - 1] \times 1000‰$. The instrumental mass fractionation factor is corrected using zircon standard Penglai with a $\delta^{18}O$ value of 5.30‰ (Li et al., 2010b). Intensities of ^{16}O were typically at the magnitude of 10^9 cps. Each analysis cost ~5 min consisting of pre-sputtering (120 s), automatic beam centering (60 s) and integration of oxygen isotopes (4 s × 20 cycles, in total 80 s). The internal precision of $^{18}O/^{16}O$ ratios was about 0.3‰ at 2 SE level. The external reproducibility of $^{18}O/^{16}O$ ratios by repeated measurements of standard zircons was better than 0.4‰. Our measurements of zircon standards 91500 and Plešovice as unknown during the course of this study yield average $\delta^{18}O$ values of 10.17 ± 0.40‰ (2 SD, $n = 38$) and 8.22 ± 0.38‰ (2 SD, $n = 48$), respectively. Both are consistent within errors with their reported values of 9.94 ± 0.10‰ (Wiedenbeck et al., 2004) and 8.19 ± 0.08‰ (2 SD, $n = 5$) (J.W. Valley's unpublished data in Fu et al., 2012).

4.2.3. SIMS U–Pb dating

A new ultra high sensitivity magnetic sector Cameca IMS 1280-HR ion microprobe was applied to date zircon at the Institute of Geology and Geophysics, Chinese Academy of Sciences, Beijing. U–Pb ratios and absolute abundances were determined relative to the standard zircon 91500 (Wiedenbeck et al., 1995) or Plešovice (Sláma et al., 2008), analyses of which were interspersed with those of unknown grains, using operating and data processing procedures similar to those described by Li et al. (2009b). The ion beam size used for U–Pb dating was 20 μm × 15 μm. Precision of $^{207}Pb/^{206}Pb$ ages was better than 0.5% for the Archean and Paleoproterozoic Kongling zircons (Table S1). Measured compositions were corrected for common Pb using measured non-radiogenic ^{204}Pb. The corrections are negligible in most cases. Our measurements of an in-house zircon standard Qinghu yielded weighted average $^{206}Pb/^{238}U$ and $^{207}Pb/^{235}U$ ages of 160.5 ± 1.4 Ma (2σ, $n = 12$) and 161.0 ± 1.6 Ma (2σ, $n = 12$), respectively, which are in good agreement with its ID-TIMS ages within errors ($^{206}Pb/^{238}U$ age = 159.38 ± 0.12 Ma and $^{207}Pb/^{235}U$ age = 159.68 ± 0.22 Ma) (Li et al., 2009b).

In order to date thin overgrowth rims, a precise zircon U–Pb dating method at a scale of <5 μm was also utilized. A finely focused, continuously variable primary O_2^- beam in Gaussian mode was used to sputter zircons generating a fat "U" shape bottom, to maximize intensity at the center. The beam intensity of ~100 pA was obtained for the Gaussian mode primary O_2^- probe by optimizing the primary column. Secondary ion optics was optimized to ensure a high Pb^+ sensitivity of 21 cps/ppm/nA with oxygen flooding technique, which is crucial to improve the precision of $^{207}Pb/^{206}Pb$ measurement. Precision and accuracy for ages of different standard zircons obtained by this small beam U–Pb dating method can be as good as 1–2% (Liu et al., 2011). In this study, zircon standard 91500 was used as external standard, while in-house standard Qinghu was used as unknown. Analyses of 91500 and Qinghu yielded condordia ages of 1058 ± 22 Ma (2σ, MSWD = 0.0101, $n = 6$) and 161.0 ± 5.3 Ma (2σ, MSWD = 2.7, $n = 3$), respectively, which are consistent with their reference ages. Analytical details were described by Liu et al. (2011). This technique has been successfully used to date small zircons from eucrite and Martian meteorite (Zhou et al., 2013a,b).

4.2.4. LA-ICP-MS U–Pb dating

U–Pb isotopes of zircons were determined by an excimer ArF GeoLas 2005 laser ablation system coupled with an Agilent 7500a ICP-MS at the State Key Laboratory of Geological Processes and Mineral Resources, China University of Geosciences, Wuhan. Detailed analytical procedures were described by Liu et al. (2010). The laser beam was typically 32 μm in diameter with a frequency of 6 Hz. Helium was used as carrier gas to provide efficient aerosol transport to the ICP and minimize aerosol deposition around the ablation site and within the transport tube (Eggins et al., 1998; Jackson et al., 2004). Two milliliters per minute of nitrogen were added to the central gas flow in LA-ICP-MS in order to increase the sensitivity of U–Th–Pb isotopes (Hu et al., 2008). The carrier and make-up gas flows were optimized by ablating NIST SRM 610 to obtain maximum signal intensity for ^{208}Pb, while keeping low ThO/Th and Ca^{2+}/Ca^+ ratios to minimize the matrix-induced interferences. Each analysis incorporated a background acquisition of 20–30 s (gas blank) followed by 50 s data acquisition from the sample. Zircon 91500 was used as external standard for U–Pb dating. Our measurements of GJ-1 yielded weighted average $^{206}Pb/^{238}U$, $^{207}Pb/^{235}U$ and $^{207}Pb/^{206}Pb$ ages of 601.6 ± 1.7 Ma (2σ, MSWD = 0.41, $n = 76$), 602.9 ± 3.4 Ma (2σ, MSWD = 0.32, $n = 76$) and 605 ± 16 Ma (2σ, MSWD = 0.30, $n = 76$), respectively, which agree within errors with its reference age of 599.8 ± 1.7 Ma (2σ) (Jackson et al., 2004).

An in-house Excel-based software ICPMSDataCal (Ver. 9.0) was used to perform off-line selection and integration of background and analyte signals, and time-drift correction and quantitative calibration for trace element analysis and U–Pb dating (Liu et al., 2008a). Common Pb correction was applied following the method

Table 1
Chemical compositions of granitic gneisses KH112 and KH110 from the Kongling Terrain.

Sample	KH112	KH110		KH112	KH110
Oxides (wt%)			Y	10.2	8.95
SiO_2	73.03	73.22	Zr	85.5	76.8
TiO_2	0.09	0.12	Nb	3.95	4.40
Al_2O_3	14.84	14.26	Cs	0.74	0.89
FeO_{total}	1.06	1.22	Ba	621	471
MnO	0.02	0.02	La	12.2	17.0
MgO	0.52	0.50	Ce	22.4	32.2
CaO	1.65	1.40	Pr	2.60	3.62
Na_2O	4.80	3.91	Nd	9.74	13.4
K_2O	3.29	4.57	Sm	2.09	2.64
P_2O_5	0.04	0.05	Eu	0.61	0.65
LOI	0.76	0.47	Gd	1.98	2.19
Total	100.10	99.74	Tb	0.29	0.29
$Mg^{\#}$	47	43	Dy	1.71	1.58
Trace element contents (ppm)			Ho	0.35	0.31
Li	9.01	8.82	Er	0.99	0.82
Be	2.06	0.95	Tm	0.14	0.12
Sc	4.04	3.08	Yb	0.92	0.78
V	12.7	12.4	Lu	0.14	0.12
Cr	6.13	7.85	Hf	2.75	2.15
Co	2.96	3.07	Ta	0.10	0.10
Ni	5.32	5.09	Pb	22.1	23.5
Cu	3.62	8.41	Th	5.44	7.17
Zn	21.8	24.9	U	0.73	0.56
Ga	17.9	17.5	Eu/Eu*	0.91	0.80
Rb	82.9	105	ΣREE	56	76
Sr	271	232	La_N/Yb_N	9	15

$Mg^{\#}$ = atomic $Mg/(Mg + Fe_{total}) \times 100$. $Eu/Eu^* = 2 \times Eu_N/(Sm_N + Gd_N)$. Normalization uses chondrite values from McDonough and Sun (1995).

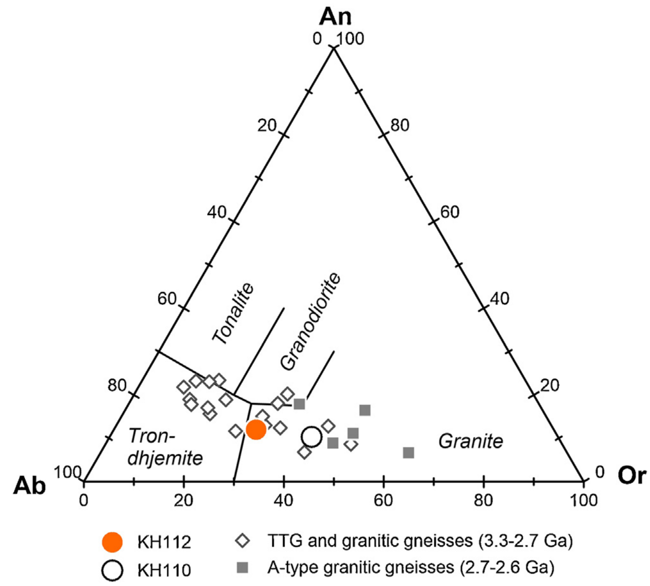

Fig. 3. Classification of Archean granitoid gneisses from the Kongling Terrain by their normative feldspar compositions (Barker, 1979). Circles represent granitic gneisses KH112 (filled) and KH110 (open) from this study. Open diamonds represent 3.3–2.7 Ga TTG and granitic gneisses (Gao et al., 1999, 2011; Chen et al., 2013). Filled squares denote 2.7–2.6 Ga A-type granitic gneisses (Gao et al., 1999; Chen et al., 2013). Ab, Or and An denote albite, orthoclase and anorthite, respectively.

of Andersen (2002). The correction was negligible in most cases. Weighted averages and intercept ages were calculated using ISOPLOT (Ver. 3.76) (Ludwig, 2012).

4.2.5. LA-MC-ICP-MS Lu–Hf isotope analysis

Analysis of zircon Hf isotopes was performed on a Neptune Plus MC-ICP-MS (Thermo Fisher Scientific, Germany) connected to a GeoLas 2005 laser system at the State Key Laboratory of Geological Processes and Mineral Resources, China University of Geosciences, Wuhan. Detailed descriptions of the technique were reported in Hu et al. (2012). Combination of a newly designed X skimmer cone with a jet sample cone was applied to the MC-ICP-MS. Four milliliters per minute of nitrogen were added to the central gas flow in LA-MC-ICP-MS in order to increase the sensitivity of Hf and suppress the non-linear mass fractionation (Hu et al., 2012). The spot size was 44 μm. Time-drift correction and external calibration were using zircon standard 91500. Measured $^{176}Hf/^{177}Hf$ ratios of standard zircons GJ-1 and Mud Tank as unknown are 0.282029 ± 0.000007 (2σ, $n = 46$) and 0.282503 ± 0.000018 (2σ, $n = 13$), which are consistent with their recommended values of 0.282015 ± 0.000019 (2 SD, $n = 25$) (Elhlou et al., 2006) and 0.282507 ± 0.000006 (2 SD, $n = 5$) (Woodhead and Hergt, 2005), respectively.

5. Results

5.1. Whole-rock chemistry

Major and trace element compositions of granitic gneisses KH112 and KH110 are listed in Table 1. They have several features in common such as (1) high SiO_2 (73 wt.%), $K_2O + Na_2O$ (>8 wt.%) and K_2O/Na_2O (0.7–1.2), (2) moderate Al_2O_3 (14–15 wt.%), and (3) very low $FeO_{total} + MgO$ (<2 wt.%). Their magnesium numbers ($100 \times$ atomic $Mg/(Mg + Fe_{total})$) are 47 and 43, respectively. Based on their normative feldspar compositions, both samples fall into the granite field (Fig. 3).

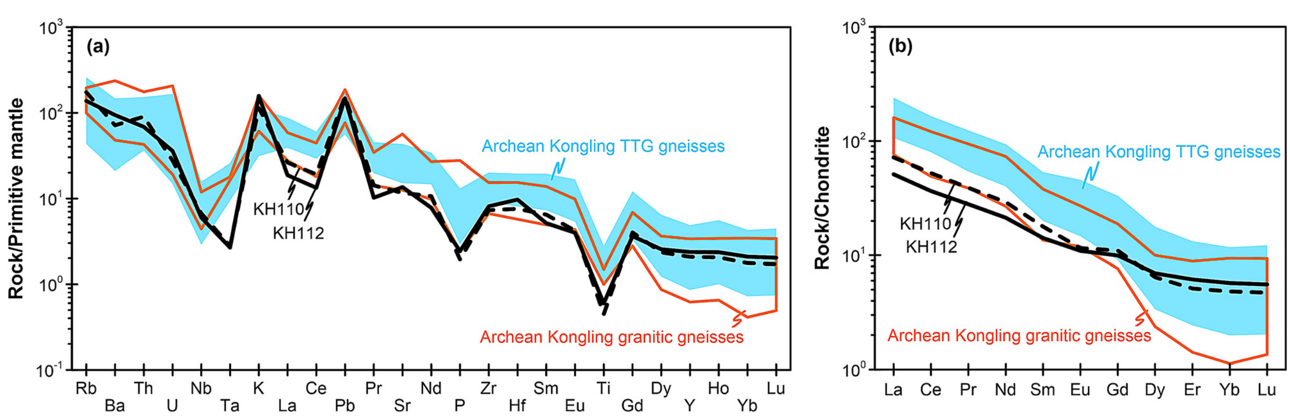

Fig. 4. (a) Primitive mantle-normalized trace element distributions and (b) chondrite-normalized rare earth element patterns of Archean granitoid gneisses from the Kongling Terrain. Solid and dashed black lines denote granitic gneisses KH112 and KH110, respectively. Filled and open areas denote Archean Kongling TTG gneisses and granitic gneisses, respectively (Gao et al., 1999, 2011; Chen et al., 2013). Primitive mantle and chondrite values used for normalization are from McDonough and Sun (1995).

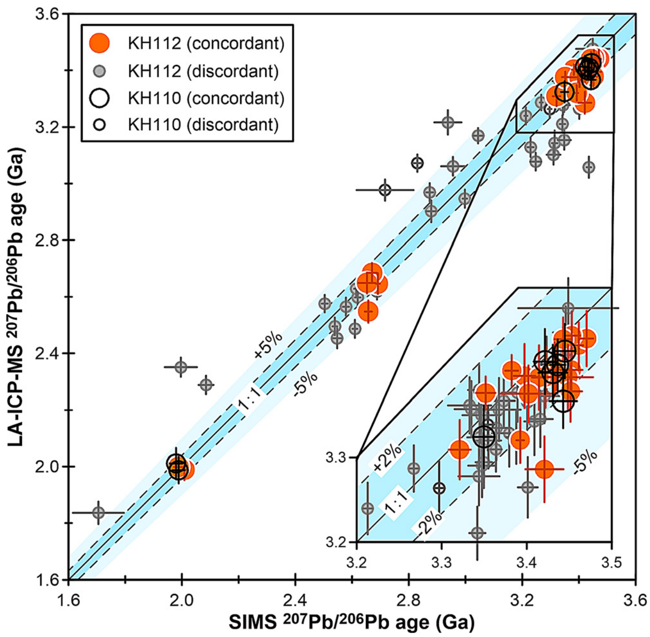

Fig. 5. Comparison of ^{207}Pb/^{206}Pb ages (n = 95) obtained by SIMS and LA-ICP-MS on the same zircon spots. The area for the 3.4–3.2 Ga zircons is enlarged. Concordant ages with 98–102% age concordance from KH112 and KH110 are shown as large filled and open circles, respectively, while small symbols denote discordant ages. Horizontal and vertical lengths of the crosses represent ±2σ errors for SIMS and LA-ICP-MS ages, respectively. It can be seen that in most cases, the SIMS and LA-ICP-MS ages agree with each other within ±2% difference for the 3.4–3.3 Ga zircons. For the younger zircons, the age difference is less than ±5%. Exceptions are some of the discordant ages. Filled areas indicate age differences within ±2% (darker) and ±5% (lighter).

Trace element compositions of the two samples show strong enrichment in large ion lithophile elements (K, Rb, Ba, Th, U, and Pb) and depletion in high field strength elements (Nb, Ta, P, and Ti) (Fig. 4a). Their total REE contents are as low as ~60 ppm with fractionated chondrite-normalized REE patterns (La_N/Yb_N = 9–15) and negative Eu anomalies (Eu/Eu* = 0.80–0.91) (Fig. 4b). They have very low Cr (<10 ppm) and Ni (~5 ppm) concentrations. Both samples are similar to the Archean TTG gneisses from the Kongling Terrain (Gao et al., 1999, 2011; Chen et al., 2013) (Fig. 4).

5.2. Zircon U–Pb ages

Zircon U–Pb–Lu–Hf–O isotopic data are given in online Supplementary Table S1. In the following text, we use ^{207}Pb/^{206}Pb ages with 98–102% age concordance, unless otherwise indicated.

For comparison, a suite of zircons from the two gneisses were dated by both SIMS and LA-ICP-MS on the same spots. The results show that in most cases, the SIMS and LA-ICP-MS ages agree with each other within ±2% (i.e., ≤70 Ma) difference for the 3.4–3.3 Ga zircons (Fig. 5). For younger zircons, the age difference is less than ±5%. Exceptions are some discordant ages (Fig. 5).

5.2.1. KH112

One hundred and five SIMS and three hundred and one LA-ICP-MS age analyses were done on KH112. Both sets of data show five concordant age groups: 3.4, 3.3, 2.9, 2.7, and 2.0 Ga (Fig. 6a and b).

The 3.4 Ga zircons can be classified into three groups based on their CL images. Group A shows a banded or linear structure, typical of magmatic zircons (Fig. 7a–c). Group B is structureless or displays weak sector zoning, characteristic of metamorphic zircons (Fig. 7d–f). Group C grows over other 3.4–3.3 Ga zircon cores as thin layers (Fig. 8), which appear to be enclosed by a 2.0 Ga rim (Fig. 8b). As discussed below, the 3.3 Ga zircons were altered from the 3.4 Ga zircons. All the three groups show similar ranges of Th/U ratios from 0.3 to 1.0 (Fig. 9). The SIMS dating yields weighted average ages of 3437 ± 12 Ma (2σ, MSWD = 13, n = 6) for Group A and 3448 ± 11 Ma (2σ, MSWD = 13, n = 11) for Group B (Fig. 10a and b). A small primary beam of <5 μm in diameter was used to date Group C. Two dates yield a weighted average age of 3479 ± 26 Ma (2σ, MSWD = 0.49, n = 2) (Fig. 10c). The LA-ICP-MS dating yields weighted average ages of 3444 ± 22 Ma (2σ, MSWD = 0.23, n = 5)

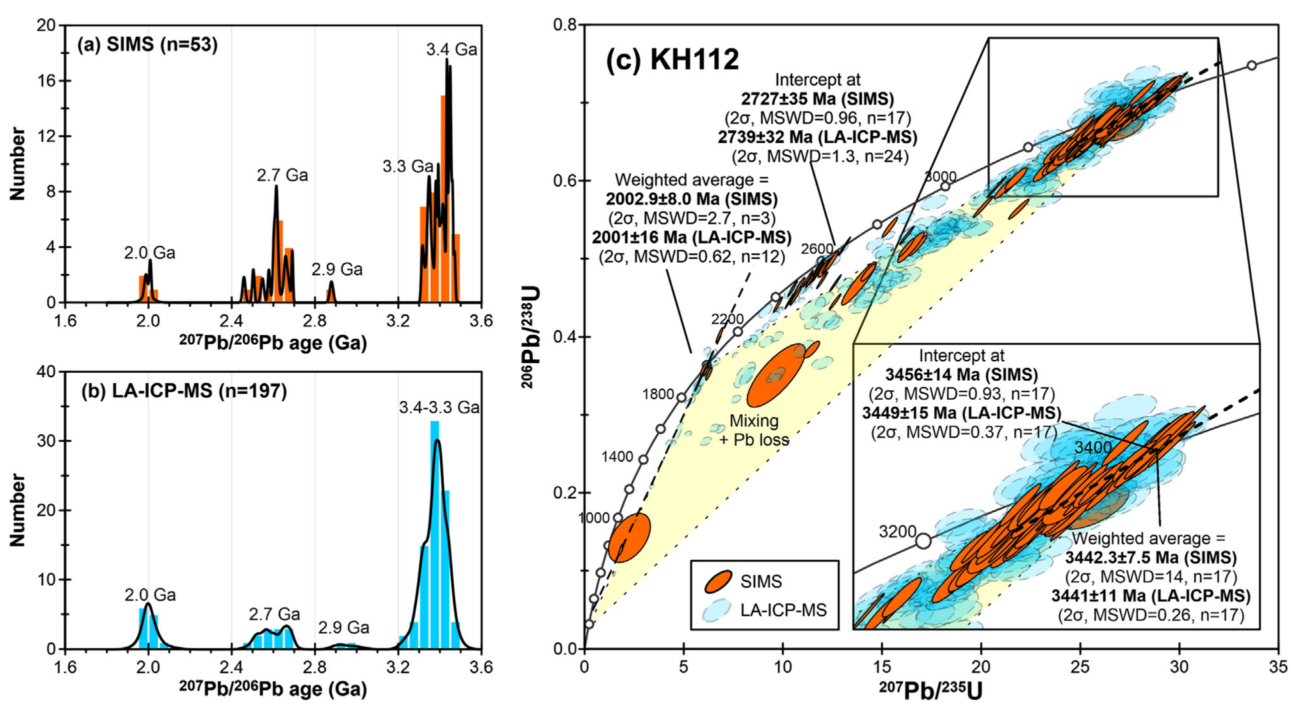

Fig. 6. Distributions of zircon ^{207}Pb/^{206}Pb ages with 98–102% age concordance for granitic gneiss KH112 determined by SIMS (a) and LA-ICP-MS (b). (c) U–Pb concordia plot. The part for the 3.4 Ga zircons is enlarged. SIMS and LA-ICP-MS U–Pb data are plotted in solid and dashed ellipses, respectively. Errors are given at 2σ level.

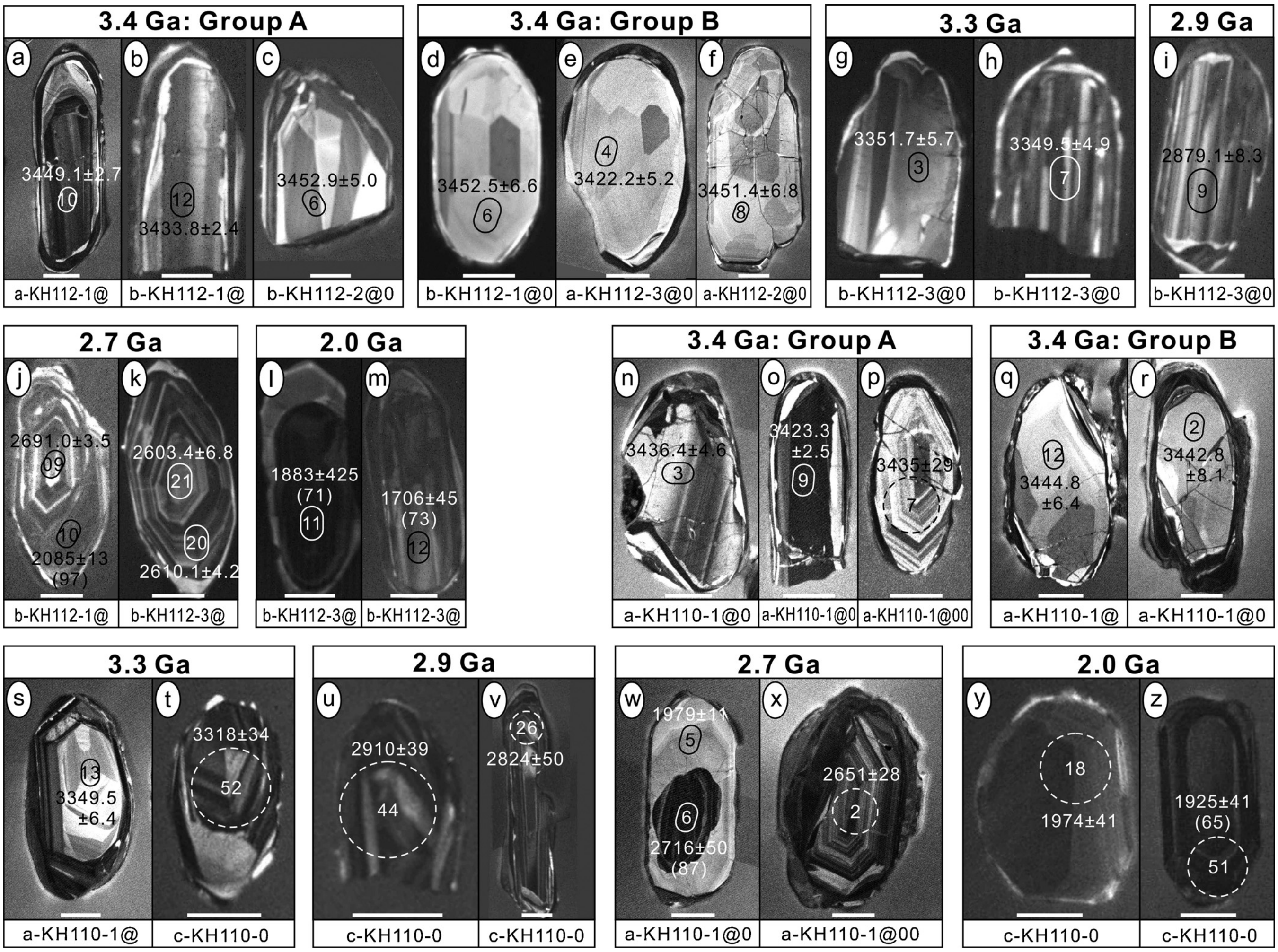

Fig. 7. Representative cathodoluminescence images of zircons from granitic gneisses KH112 (a–m) and KH110 (n–z). Solid ellipses represent SIMS craters (20 μm × 15 μm), while dashed circles denote LA-ICP-MS spots (32 μm in diameter). Numbers in the center of the ellipses or circles are analytical numbers with their prefixes listed at the bottom of each CL image. $^{207}Pb/^{206}Pb$ ages are shown with 1σ errors in Ma. Age concordance is 98–102%, unless otherwise indicated in the parentheses. White bars correspond to a length of 30 μm.

and 3440 ± 12 Ma (2σ, MSWD = 0.29, *n* = 12) for Groups A and B, respectively (Fig. 10d and e). Group C is too thin to be dated by LA-ICP-MS. Groups A and B together give weighted average ages of 3442.3 ± 7.5 Ma (2σ, MSWD = 14, *n* = 17) for SIMS and 3441 ± 11 Ma (2σ, MSWD = 0.26, *n* = 17) for LA-ICP-MS (Fig. 6c). They yield upper intercept ages of 3456 ± 14 Ma (2σ, MSWD = 0.93, *n* = 17) for SIMS and 3449 ± 15 Ma (2σ, MSWD = 0.37, *n* = 17) for LA-ICP-MS (Fig. 6c).

Most of the 3.3 Ga zircons have banded, linear or oscillatory zoning patterns, typical of magmatic zircons (Fig. 7g and h). The SIMS dating yields a weighted average age of 3373 ± 13 Ma (2σ, MSWD = 29, *n* = 18). The LA-ICP-MS dating yields a weighted average age of 3368.3 ± 8.9 Ma (2σ, MSWD = 2.6, *n* = 61).

The 2.9 Ga zircons are rare. They are elongate prismatic (aspect ratios = 2–5), showing linear zoning, indicative of a magmatic origin (Fig. 7i). One SIMS date has an age of 2879.1 ± 8.3 Ma (1σ, *n* = 1), while two LA-ICP-MS dates yield a weighted average age of 2939 ± 52 Ma (2σ, MSWD = 2.0, *n* = 2).

The 2.7 Ga zircons are short prismatic with aspect ratios of 2–3, exhibiting broad to fine concentric oscillatory zoning patterns, typical of magmatic zircons (Fig. 7j and k). The SIMS dating gives a weighted average age of 2617 ± 31 Ma (2σ, MSWD = 98, *n* = 13). Most of the SIMS dates are slightly discordant and they follow a Pb-loss trend toward ca. 2.0 Ga. Together with the 2.0 Ga zircons, they yield an upper intercept age of 2727 ± 35 Ma (2σ, MSWD = 0.96, *n* = 17). Comparably, the LA-ICP-MS dating yields a weighted average age of 2607 ± 39 Ma (2σ, MSWD = 9.3, *n* = 12) and an upper intercept age of 2739 ± 32 Ma (2σ, MSWD = 1.3, *n* = 24).

The 2.0 Ga zircons are structureless and metamict in CL images (Fig. 7l and m). Most of their Th/U ratios are below 0.4 (Fig. 9). These two features characterize metamorphic zircons. They have high U contents (up to 2000 ppm) (Table S1) and are commonly discordant (Fig. 6c). The SIMS and LA-ICP-MS dating yield weighted average ages of 2002.9 ± 8.0 Ma (2σ, MSWD = 2.7, *n* = 3) and 2001 ± 16 Ma (2σ, MSWD = 0.62, *n* = 12), respectively (Fig. 6c). Such ages also dominate the metamorphic overgrowth rims on the Archean zircons.

5.2.2. KH110

Thirteen SIMS and one hundred and ninety LA-ICP-MS age analyses were done on KH110. The SIMS and LA-ICP-MS data show similar five concordant age groups: 3.4, 3.3, 2.9, 2.7 and 2.0 Ga (Fig. 11a and b). Like KH112, the 3.4 Ga zircons in KH110 can also be classified into Groups A (magmatic, Fig. 7n–p) and B (metamorphic, Fig. 7q and r). The overgrowth rims were not analyzed. Groups A and B show similar Th/U ratios (Fig. 9b) and ages (Fig. 10f–i) as well. The SIMS dating yields weighted average ages of 3426 ± 69 Ma (2σ, MSWD = 6.4, *n* = 2) and 3434.9 ± 7.2 Ma (2σ, MSWD = 2.6, *n* = 4) for Groups A and B, respectively (Fig. 10f and g). The LA-ICP-MS dating

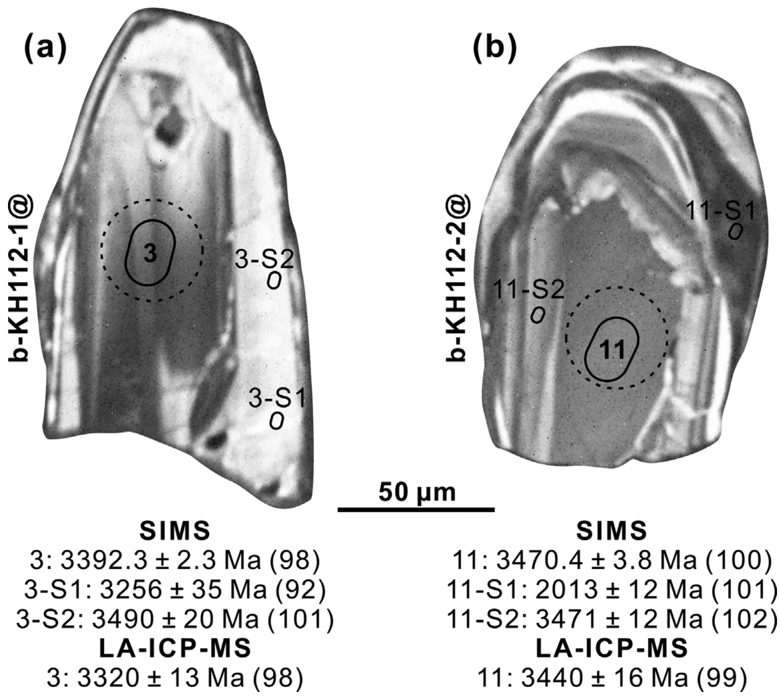

Fig. 8. Comparison of SIMS and LA-ICP-MS $^{207}Pb/^{206}Pb$ ages on the same 3.3 Ga (a) and 3.4 Ga (b) zircon spots. Solid ellipses and dashed circles represent SIMS craters (20 μm × 15 μm) and LA-ICP-MS spots (32 μm in diameter), respectively. Also shown are SIMS ages of overgrowth rims determined by a small ion beam of <5 μm in diameter. Numbers in the center of the ellipses or around the circles are analytical numbers with their prefixes listed at the left of each CL image. Age errors are given at 1σ level. Numbers in the parentheses are age concordance in %. As discussed in the text, the 3.3 Ga zircons were altered from the 3.4 Ga zircons. This is supported by the older overgrowth rim (b-KH112-1@3-S2) in (a).

yields weighted average ages of 3437 ± 39 Ma (2σ, MSWD = 0.005, n = 2) for Group A and 3422 ± 22 Ma (2σ, MSWD = 0.47, n = 4) for Group B (Fig. 10h and i). These two groups together give weighted average ages of 3428.5 ± 9.2 Ma (2σ, MSWD = 3.7, n = 6) for SIMS and 3425 ± 19 Ma (2σ, MSWD = 0.37, n = 6) for LA-ICP-MS (Fig. 11c). They yield upper intercept ages of 3481 ± 170 Ma (2σ, MSWD = 0.94, n = 6) for SIMS and 3423 ± 25 Ma (2σ, MSWD = 0.78, n = 6) for LA-ICP-MS (Fig. 11c).

The 3.3 Ga zircons mainly have low luminance in CL images with linear or oscillatory zoning patterns, typical of magmatic zircons (Fig. 7s and t). The SIMS dating yields one concordant age of 3349.5 ± 6.4 Ma (1σ, n = 1), while the LA-ICP-MS dating yields a weighted average age of 3359 ± 16 Ma (2σ, MSWD = 2.3, n = 25).

The 2.9 Ga zircons show oscillatory zoning of magmatic zircons (Fig. 7u and v). Only two grains were identified by LA-ICP-MS, which give a weighted average age of 2877 ± 61 Ma (2σ, MSWD = 1.9, n = 2).

The 2.7 Ga zircons are generally short prismatic, showing concentric oscillatory zoning, typical of magmatic zircons (Fig. 7w and x). No 2.7 Ga zircons were dated by SIMS. The LA-ICP-MS dating reveals a weighted average age of 2635 ± 30 Ma (2σ, MSWD = 0.51, n = 3). Like in KH112, together with the 2.0 Ga zircons, they yield an upper intercept age of 2729 ± 120 Ma (2σ, MSWD = 2.6, n = 41) (Fig. 11c).

The 2.0 Ga zircons are more abundant in KH110 than those in KH112, but they show similar age and chemical features (Fig. 7y

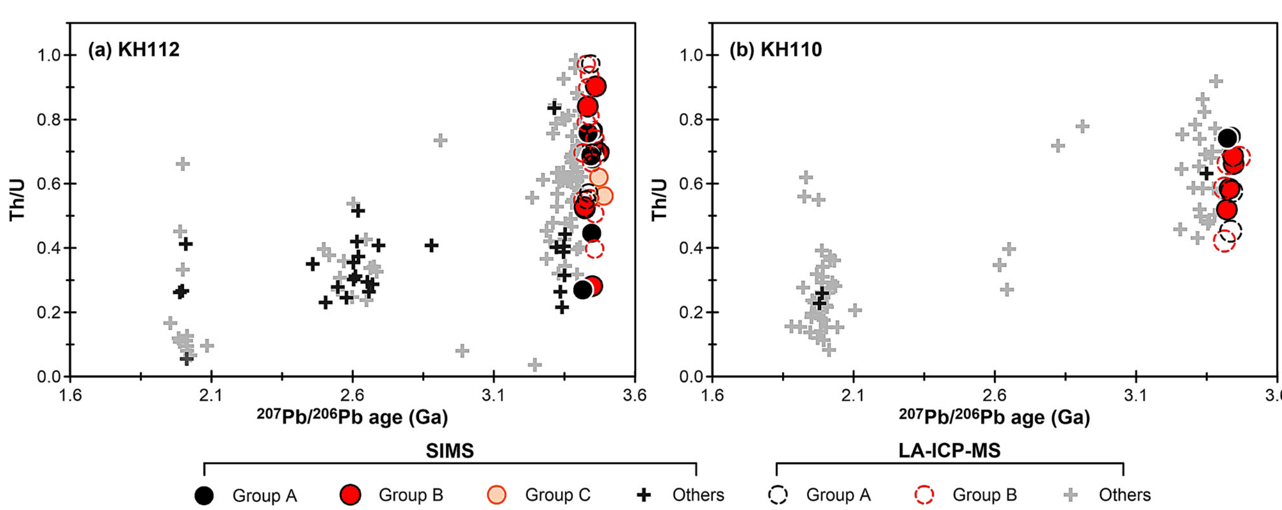

Fig. 9. Th/U ratio versus $^{207}Pb/^{206}Pb$ age of zircons with 98–102% age concordance from granitic gneisses KH112 (a) and KH110 (b). Filled circles and black crosses indicate SIMS data, while open circles and gray crosses represent LA-ICP-MS data.

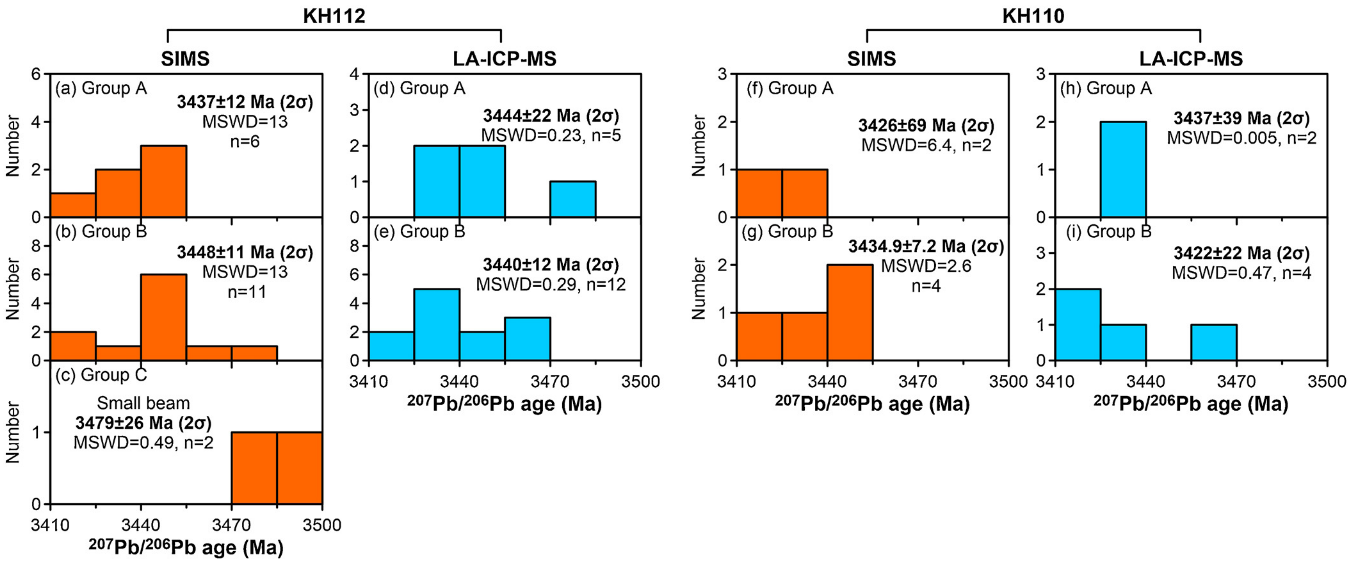

Fig. 10. Distributions of $^{207}Pb/^{206}Pb$ ages of the 3.4 Ga zircons (Groups A, B, and C) with 98–102% age concordance from granitic gneisses KH112 (a–e) and KH110 (f–i). For either sample, data obtained by SIMS and LA-ICP-MS are shown at the left and right panels, respectively. Numbers are weighted average ages with 2σ errors. Group C was too thin to be analyzed by LA-ICP-MS.

and z). The SIMS and LA-ICP-MS dating yield weighted average ages of 1984 ± 16 Ma (2σ, MSWD = 0.34, n = 2) and 2018 ± 12 Ma (2σ, MSWD = 2.3, n = 37), respectively (Fig. 11c). The upper intercept age for LA-ICP-MS is 1993 ± 13 Ma (2σ, MSWD = 0.82, n = 38), whereas too few analyses were available for SIMS to yield an upper intercept age.

5.3. Zircon Hf isotopes

Zircon Lu–Hf isotopic data are given in Table S1, where $^{176}Hf/^{177}Hf$ (t) ratios were calculated back to the $^{207}Pb/^{206}Pb$ ages using their measured values. The ε_{Hf} value was calculated with reference to a chondritic reservoir (CHUR). $^{176}Lu/^{177}Hf$ and $^{176}Hf/^{177}Hf$ values used for the CHUR are 0.0336 and 0.282785, respectively (Bouvier et al., 2008). A decay constant of 1.867×10^{-5} Ma^{-1} (Söderlund et al., 2004) was used for ^{176}Lu. The single-stage model age (T_{DM1}) was calculated relative to the depleted mantle with a present-day $^{176}Hf/^{177}Hf$ of 0.28325 and $^{176}Lu/^{177}Hf$ of 0.0384 (Griffin et al., 2002). The two-stage model age (T_{DM2}), which is interpreted as crust formation age, was calculated by projecting the zircon $^{176}Hf/^{177}Hf$ (t) back to the depleted-mantle model growth curve assuming a $^{176}Lu/^{177}Hf$ ratio

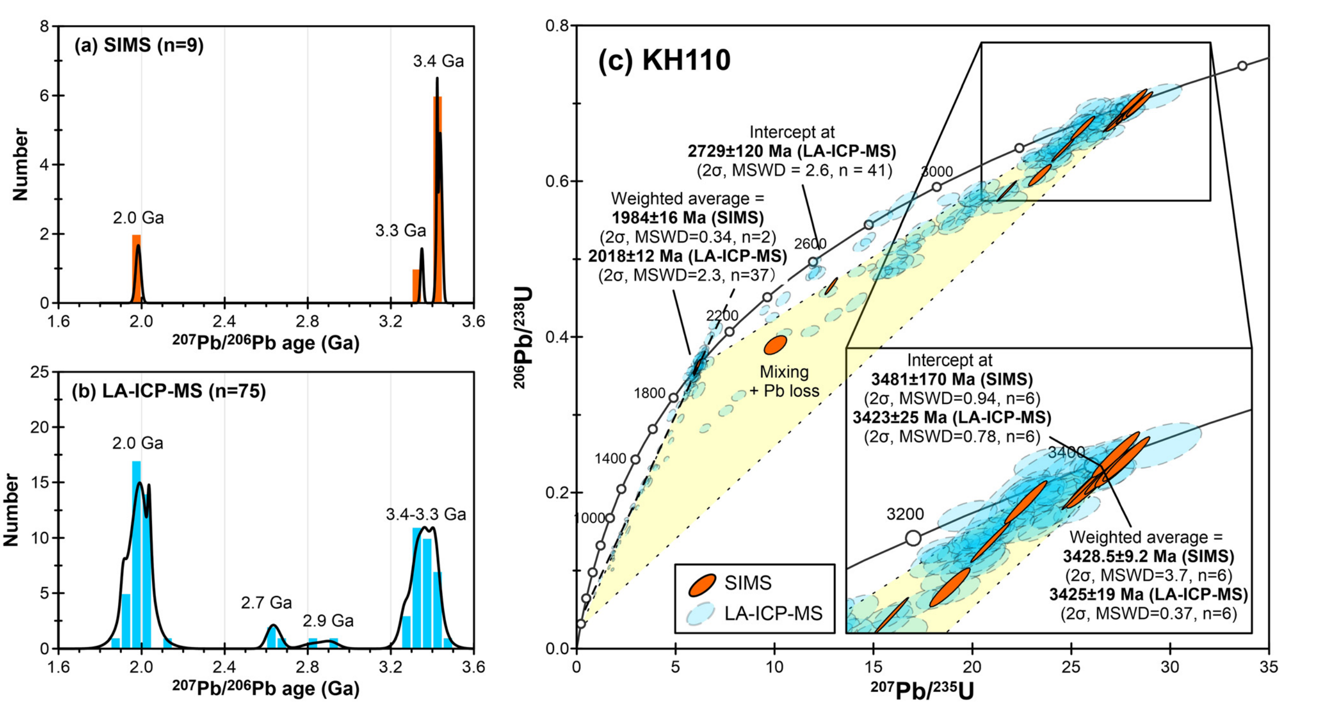

Fig. 11. Distributions of zircon $^{207}Pb/^{206}Pb$ ages with 98–102% age concordance for granitic gneiss KH110 determined by SIMS (a) and LA-ICP-MS (b). (c) U–Pb concordia plot. The part for the 3.4 Ga zircons is enlarged. SIMS and LA-ICP-MS U–Pb data are plotted in solid and dashed ellipses, respectively. The upper intercept age for SIMS is not calculated because few analyses are available. Errors are given at 2σ level.

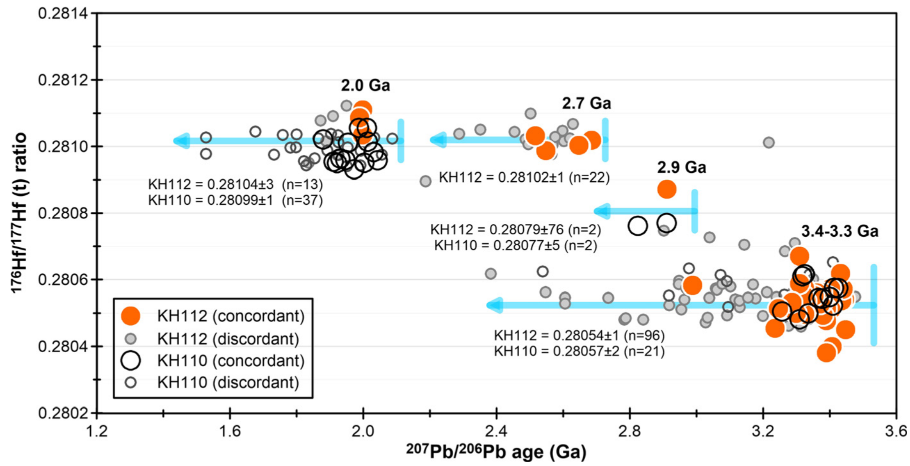

Fig. 12. ^{176}Hf/^{177}Hf (t) ratio versus ^{207}Pb/^{206}Pb age of zircons from granitic gneisses KH112 (filled circles) and KH110 (open circles). Large symbols indicate concordant zircons (with 98–102% age concordance) and small symbols represent discordant zircons. The ^{176}Hf/^{177}Hf ratio was calculated back to its corresponding ^{207}Pb/^{206}Pb age. Numbers are weighted average ^{176}Hf/^{177}Hf (t) ratios with 2σ errors calculated for each group that includes both concordant and discordant zircons with similar ^{176}Hf/^{177}Hf (t) ratios.

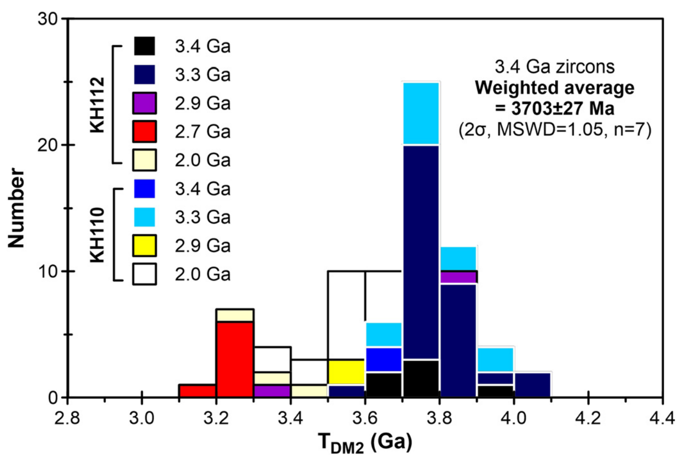

Fig. 13. Histograms of two-stage Hf model ages (T_{DM2}) for zircons with 98–102% age concordance from granitic gneisses KH112 and KH110. The number is the weighted average T_{DM2} for 3.4 Ga zircons from both samples.

of 0.0093 for the upper continental crust (Vervoort and Patchett, 1996).

Lu–Hf isotopes of one hundred and forty-one zircons from KH112 and sixty from KH110 were analyzed. As illustrated in Fig. 12, ^{176}Hf/^{177}Hf (t) ratios of both concordant and discordant zircons show three distinctly different groups with ^{207}Pb/^{206}Pb ages of 3.4–2.4, 2.9–2.8, and 2.7–1.5 Ga. Each group has a similar ^{176}Hf/^{177}Hf (t) ratio for both granitic gneisses, which varies from 0.28054–0.28057 for 3.4–2.4 Ga through 0.28077–0.28079 for 2.9–2.8 Ga to 0.28099–0.28104 for 2.7–1.5 Ga (Fig. 12). Concordant zircons from the two granitic gneisses exhibit similar T_{DM2} distributions, which range from 4.1 to 3.2 Ga (Fig. 13). Taken together, the 3.4 Ga zircons of the two samples have T_{DM2} ages ranging from 3.9 to 3.6 Ga with a weighted average of 3703 ± 27 Ma (2σ, MSWD = 1.05, n = 7) (Fig. 13).

5.4. Zircon O isotopes

Forty-eight and Forty-seven zircons from KH110 and KH112 were analyzed for oxygen isotopes, respectively (Table S1). Twelve from KH112 and twenty one from KH110 have age concordance between 98% and 102%. Zircon oxygen isotopes of the two granitic gneisses vary widely. δ^{18}O values of the Archean zircons range from 5.4 to 6.8‰, covering mantle to supracrustal values (Valley et al., 1998, 2005) (Fig. 14a). The Proterozoic zircons display an even larger variation from 3.1 to 7.5‰ in δ^{18}O (Fig. 14b). There is an apparent positive correlation between δ^{18}O and age concordance for the Proterozoic zircons with a correlation coefficient R^2 of 0.7297 (Fig. 14b). In contrast, the Archean zircons do not exhibit such a correlation (R^2 = 0.001).

6. Discussion

6.1. The oldest rocks in South China

As described above, the two granitic gneisses exhibit similar age patterns. Furthermore, all the three groups of the 3.4 Ga zircons in the two samples have similar ranges in Th/U ratio (Fig. 9). Their ages are identical within 2σ errors (Fig. 10). The CL images and Th/U ratios of Group A agree with a magmatic origin. The CL images of Groups B and C are typically metamorphic, which appear to be in conflict with their high Th/U ratios. There are two possible scenarios for the genesis of Groups B and C. On one hand, they may also have an igneous origin. In this case, later metamorphism must have modified their CL images but kept their Th/U ratios largely intact. Although Group C was too thin to be analyzed by LA-MC-ICP-MS, Groups A (^{176}Hf/^{177}Hf (t) = 0.280520 ± 0.000010, 2σ, n = 3) and B (^{176}Hf/^{177}Hf (t) = 0.280572 ± 0.000016, 2σ, n = 5) have nearly identical ^{176}Hf/^{177}Hf (t) ratios. This suggests that Groups A and B were derived from the same source. On the other hand, Groups B and C may be metamorphic in origin. Previous studies show that metamorphic zircons from granulite could have Th/U ratios as high (0.3–1.0) as magmatic zircons (Hoskin and Black, 2000; Siebel et al., 2012). This is supported by locally preserved mafic granulite in the Kongling Terrain, which usually occurs as lens, boudins, and layers in the felsic gneisses (Gao et al., 1999). In any case, the metamorphic event must have occurred after the granitic magmatism within a few tens of million years, as constrained by the 2σ age errors of Groups A and B (Fig. 10).

The two granitic gneisses show indistinguishable age patterns for the 3.4 Ga zircons. Taken together, the SIMS data of the two samples give weighted average ages of 3434.3 ± 9.6 Ma (2σ, MSWD = 13, n = 8) for Group A and 3446.0 ± 8.8 Ma (2σ, MSWD = 10.7, n = 15) for Group B. Groups A and B together yield an upper intercept age of 3457 ± 14 Ma (2σ, MSWD = 0.85, n = 23). The LA-ICP-MS data yield weighted average ages of 3442 ± 19 Ma (2σ, MSWD = 0.17, n = 7) for Group A and 3435 ± 11 Ma (2σ, MSWD = 0.44, n = 16) for Group B. They yield an upper intercept age of 3443 ± 13 Ma (2σ,

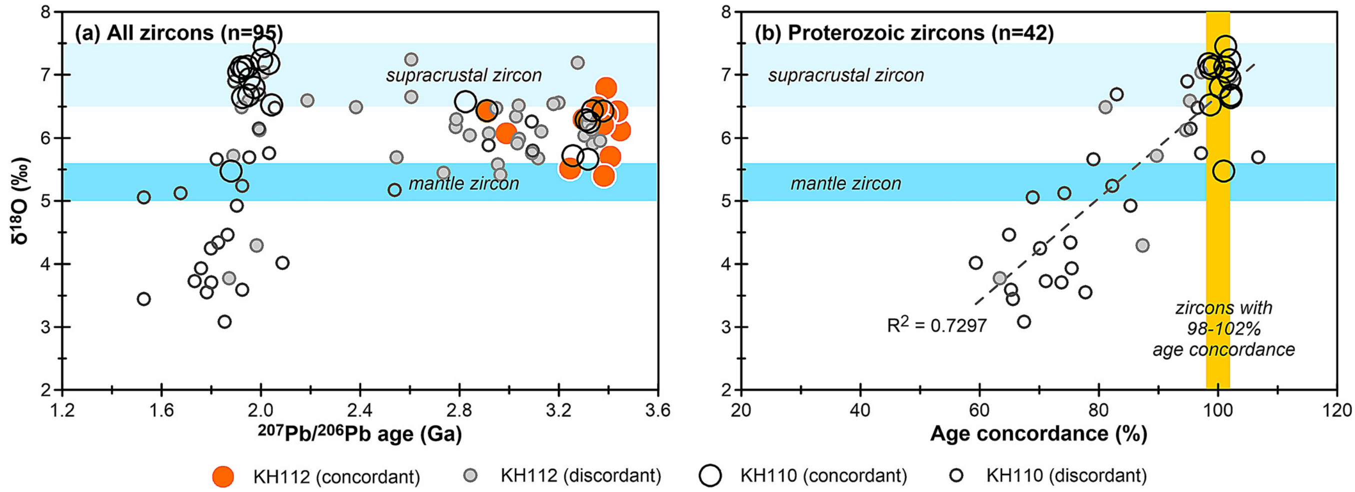

Fig. 14. Variation of $\delta^{18}O$ value against (a) $^{207}Pb/^{206}Pb$ age for all zircons and (b) age concordance for Proterozoic zircons from granitic gneisses KH112 (filled circles) and KH110 (open circles). Ranges of mantle (5.3 ± 0.3‰) and supracrustal (6.5–7.5‰) zircons are from Valley et al. (1998, 2005).

MSWD = 0.63, n = 23). These SIMS and LA-ICP-MS ages are consistent. Comparison between SIMS and LA-ICP-MS zircon U–Pb ages is shown in Figs. 5 and 10 and is discussed in Supplementary online materials.

We propose that the above SIMS and LA-ICP-MS ages of Groups A and B are the best estimates of the granitic magmatism and the subsequent metamorphism. The small-beam SIMS ages of Group C are not considered due to their large analytical errors. Accordingly, these two granitic gneisses represent the oldest rocks currently known in South China (Fig. 15). They predate the 3300-Ma-old trondhjemitic gneiss from the Kongling Terrain by 150 Ma (Gao et al., 2011).

The 3.4 Ga magmatic zircons show near chondritic ε_{Hf} (t) ($-0.7 \pm 1.0, 2\sigma$, MSWD = 1.14, n = 8), which is below the coeval value of the depleted mantle (+5.2) (Fig. 16), from which the new crust is assumed to be derived (Griffin et al., 2002). This suggests that the granitic magma contained materials of pre-existing continental crust. The higher-than-mantle $\delta^{18}O$ values (6.1–6.4‰) of the 3.4 Ga zircons (Fig. 14a) imply that such materials must have been interacted with surface water (e.g., Mojzsis et al., 2001; Cavosie et al., 2005). Their crust formation ages (T_{DM2}) vary from 3.9 to 3.6 Ga with a weighted average of 3703 ± 27 Ma (2σ, MSWD = 1.05, n = 7) (Fig. 13). Our results support previous studies that the Yangtze Craton may have contained the continental crust as old as 3.8 Ga (Zhang et al., 2006c; Gao et al., 2011).

6.2. Multiple stages of later magmatism and metamorphism

Three lines of evidence suggest that the 3.3 Ga zircons were altered from the 3.4 Ga zircons. Firstly, these 3.3 Ga zircons are slightly metamict (e.g., Fig. 7h) or partially recrystallized (e.g., Fig. 7t). Secondly, they have Th/U ratios, O and particularly Lu–Hf isotopic compositions that are indistinguishable from the 3.4 Ga zircons (Figs. 8, 11 and 13). As illustrated by numerous studies, although ancient Pb loss in zircons may cause variations in their $^{207}Pb/^{206}Pb$ ages, their $^{176}Hf/^{177}Hf$ (t) ratios are immune to later alteration (e.g., Amelin et al., 2000; Gerdes and Zeh, 2009; Chen et al., 2010; Souders et al., 2013). Finally, the 3.3 Ga zircons can be observed to be overgrown by a 3.4 Ga rim (Fig. 8a).

The 2.9 Ga and 2.7 Ga zircons in both samples are rare and magmatic in origin. Their $^{176}Hf/^{177}Hf$ (t) ratios are distinct from the 3.4 Ga zircons (Fig. 12), indicating different sources. It is inferred that they were derived from injected magmas, as commonly assumed for ancient orthogneisses (e.g., Bowring and Williams, 1999; Nutman et al., 2000, 2009). The 2.9 Ga magmatism is well documented by TTG, granitic and dioritic gneisses in the Kongling Terrain (Gao et al., 1999, 2011; Qiu et al., 2000; Zhang et al., 2006a; Chen et al., 2013) and its adjacent regions (Zheng et al., 2006a; Sun et al., 2008; Wu et al., 2008). The 2.7 Ga magmatism produced A-type granite in the central Yangtze Craton with a significant

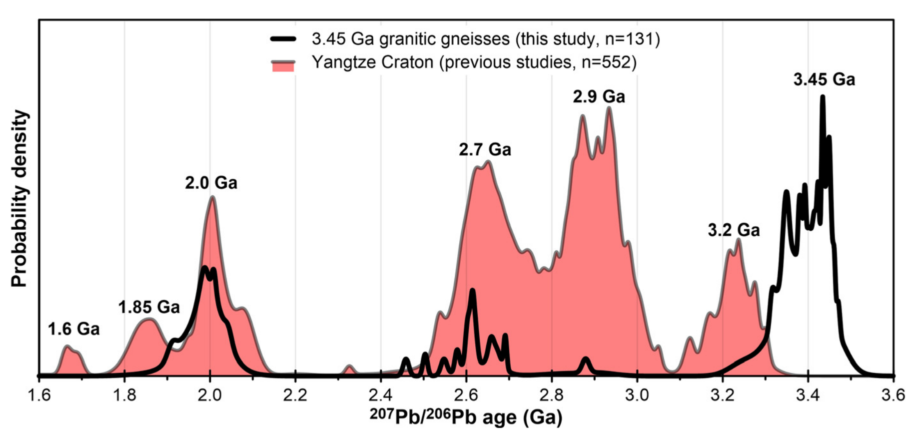

Fig. 15. Relative probability plot of zircon $^{207}Pb/^{206}Pb$ ages with 98–102% age concordance obtained for granitic gneisses KH112 and KH110 in this study (bold solid line) compared to zircons from Precambrian rocks of the Yangtze Craton from previous studies (filled area) (Qiu et al., 2000; Zhang et al., 2006a,b; Greentree and Li, 2008; Jiao et al., 2009; Wu et al., 2009, 2012; Gao et al., 2011; Peng et al., 2012; Chen et al., 2013; Wang et al., 2013).

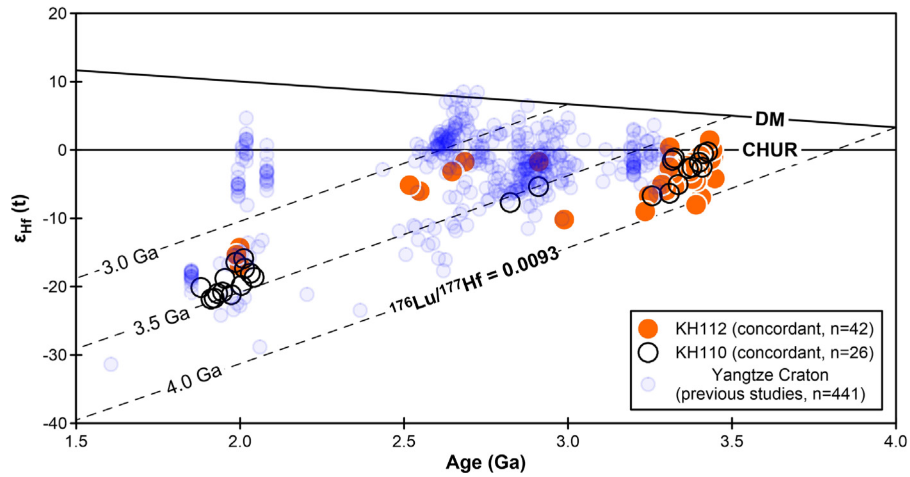

Fig. 16. Plot of ε_{Hf} (t) versus $^{207}Pb/^{206}Pb$ age of zircons with 98–102% age concordance from granitic gneisses KH112 (filled large circles) and KH110 (open large circles) compared to Precambrian zircons of the Yangtze Craton from previous studies (small circles) (Zhang et al., 2006a,b; Zheng et al., 2006a; Jiao et al., 2009; Wu et al., 2009, 2012; Gao et al., 2011; Peng et al., 2012; Chen et al., 2013). The depleted mantle (DM) evolution line is from Griffin et al. (2002).

proportion of new crustal additions, which coevals with one of the worldwide continental crustal growth episodes (Chen et al., 2013).

The 2.0 Ga metamorphic zircons are commonly high in U content (up to 2000 ppm) (Table S1) and metamict (Fig. 7i, m, y and z). Regardless of being concordant or not, they have $^{176}Hf/^{177}Hf$ (t) ratios overlapping those of the 2.7 Ga zircons (Fig. 12), suggesting a common source. In great contrast, their $\delta^{18}O$ values are strongly variable and positively correlated with age concordance (Fig. 14b). The low $\delta^{18}O$ (down to 3.1‰) requires interaction with hydrothermal fluid. These results suggest that at least some of the 2.0 Ga zircons were likely to have been altered from the 2.7 Ga zircons by hydrothermal fluid.

7. Conclusions

The two granitic gneisses from the Kongling Terrain show similar five zircon age groups of 3.4, 3.3, 2.9, 2.7, and 2.0 Ga. The 3.4 Ga zircons of the two samples give weighted average SIMS ages of 3434.3 ± 9.6 Ma (2σ, MSWD = 13, n = 8) for Group A and 3446.0 ± 8.8 Ma (2σ, MSWD = 10.7, n = 15) for Group B. Groups A and B together yield an upper intercept age of 3457 ± 14 Ma (2σ, MSWD = 0.85, n = 23). The LA-ICP-MS data yield weighted average ages of 3442 ± 19 Ma (2σ, MSWD = 0.17, n = 7) for Group A and 3435 ± 11 Ma (2σ, MSWD = 0.44, n = 16) for Group B. They yield an upper intercept age of 3443 ± 13 Ma (2σ, MSWD = 0.63, n = 23). The SIMS and LA-ICP-MS ages agree well with each other. These ages for Groups A and B are the best estimates of the granitic magmatism and the subsequent metamorphism. The metamorphism must have occurred after the granitic magmatism within a few tens of million years, as constrained by their age errors. Accordingly, these two granitic gneisses represent the oldest rocks currently known in South China, which predate the 3300-Ma-old trondhjemitic gneiss from the Kongling Terrain by 150 Ma.

The 3.4 Ga zircons show near chondritic ε_{Hf} (t) (−0.7 ± 1.0, 2σ, MSWD = 1.14, n = 8), which is below the coeval value of the depleted mantle. This suggests that the granitic magma contained materials of pre-existing continental crust. Their higher-than-mantle $\delta^{18}O$ values (6.1–6.4‰) imply that such materials must have been interacted with surface water. Their crust formation ages (T_{DM2}) vary from 3.9 to 3.6 Ga with a weighted average of 3703 ± 27 Ma (2σ, MSWD = 1.05, n = 7). Our results support previous studies that the Yangtze Craton may have contained the continental crust as old as 3.8 Ga.

Among the younger age groups, the 3.3 Ga zircons exhibit $^{176}Hf/^{177}Hf$ (t), $\delta^{18}O$ and Th/U values similar to the 3.4 Ga zircons. This suggests that the 3.3 Ga zircons were altered from the 3.4 Ga zircons. The 2.9 and 2.7 Ga zircons in both samples are rare and magmatic. Their $^{176}Hf/^{177}Hf$ (t) ratios are distinct from the 3.4 Ga zircons, indicating different sources. These two age groups are consistent with the 2.9 Ga TTG and the 2.7 Ga A-type granitic magmatism in the Yangtze Craton. Regardless of being concordant or discordant, the 2.0 Ga metamorphic zircons have $^{176}Hf/^{177}Hf$ (t) ratios overlapping those of the 2.7 Ga zircons, suggesting a common source. This is in great contrast to the positive correlation between age concordance and $\delta^{18}O$ of the 2.0 Ga zircons. The low $\delta^{18}O$ (down to 3.1‰) requires interaction with hydrothermal fluid. These results suggest that at least some of the 2.0 Ga zircons were likely to have been altered from the 2.7 Ga zircons by hydrothermal fluid.

Acknowledgements

We would like to thank Jian-Qi Wang for whole-rock major element analysis, Tao Luo, Li-Xu Deng, and Peng-Yuan Han for help in LA-ICP-MS U–Pb and LA-MC-ICP-MS Lu–Hf analysis, Hu-Jun Gong and Lu Wang for help in CL imaging, and Xian-Hua Li, Qiu-Li Li and other colleagues from IGGCAS for help in SIMS U–Pb and O analysis. We acknowledge the constructive reviews from two anonymous reviewers, which have improved this paper significantly. We finally thank Guochun Zhao for editorial handling. This research was supported by the National Nature Science Foundation of China (40973020, 41173016, and 41373026) and Chinese Ministry of Education (B07039), the Fundamental Research Funds for National Universities, as well as special funds from the State Key Laboratory of Geological Processes and Mineral Resources and from the State Key Laboratory of Continental Dynamics.

Appendix A. Supplementary data

Supplementary data associated with this article can be found, in the online version, at http://dx.doi.org/10.1016/j.precamres.2013.12.018, including zircon U–Pb–Lu–Hf–O data and a comparison between SIMS and LA-ICP-MS zircon U–Pb ages.

References

Andersen, T., 2002. Correction of common lead in U–Pb analyses that do not report ^{204}Pb. Chemical Geology 192, 59–79.

Amelin, Y., Lee, D.C., Halliday, A.N., 2000. Early-middle Archaean crustal evolution deduced from Lu–Hf and U–Pb isotopic studies of single zircon grains. Geochimica et Cosmochimica Acta 64, 4205–4225.

Armstrong, R.L., Harmon, R.S., 1981. Radiogenic isotopes: the case for crustal recycling on a near-steady-state no-continental-growth earth [and discussion]. Philosophical Transactions of the Royal Society of London. Series A: Mathematical and Physical Sciences 301, 443–472.

Barker, F., 1979. Trondhjemite: definition environment and hypotheses of origin. In: Barker, F. (Ed.), Trondhjemites, Dacites and Related Rocks. Elsevier, Amsterdam, pp. 1–12.

Bell, E.A., Harrison, T.M., McCulloch, M.T., Young, E.D., 2011. Early Archean crustal evolution of the Jack Hills zircon source terrane inferred from Lu–Hf, ^{207}Pb/^{206}Pb, and δ^{18}O systematics of Jack Hills zircons. Geochimica et Cosmochimica Acta 75, 4816–4829.

Bouvier, A., Vervoort, J.D., Patchett, P.J., 2008. The Lu–Hf and Sm–Nd isotopic composition of CHUR: constraints from unequilibrated chondrites and implications for the bulk composition of terrestrial planets. Earth and Planetary Science Letters 273, 48–57.

Bowring, S.A., Williams, I.S., 1999. Priscoan (4.00–4.03 Ga) orthogneisses from northwestern Canada. Contributions to Mineralogy and Petrology 134, 3–16.

Cavosie, A.J., Valley, J.W., Wilde, S.A., E.I.M.F, 2005. Magmatic δ^{18}O in 4400–3900 Ma detrital zircons: a record of the alteration and recycling of crust in the Early Archean. Earth and Planetary Science Letters 235, 663–681.

Cawood, P.A., Hawkesworth, C.J., Dhuime, B., 2012. The continental record and the generation of continental crust. Geological Society of America Bulletin 125, 14–32.

Chen, K., Gao, S., Wu, Y.B., Guo, J.L., Hu, Z.C., Liu, Y.S., Zong, K.Q., Liang, Z.W., Geng, X.L., 2013. 2.6-2.7 Ga crustal growth in Yangtze Craton, South China. Precambrian Research 224, 472–490.

Chen, R.-X., Zheng, Y.-F., Xie, L., 2010. Metamorphic growth and recrystallization of zircon: distinction by simultaneous in-situ analyses of trace elements, U–Th–Pb and Lu–Hf isotopes in zircons from eclogite-facies rocks in the Sulu orogen. Lithos 114, 132–154.

Condie, K.C., 2007. Chapter 1.2 The distribution of Paleoarchean crust. In: van Kranendonk, M.J., Smithies, R.H., Vickie, C.B. (Eds.), Developments in Precambrian Geology. Elsevier, Amsterdam, pp. 9–18.

Eggins, S.M., Kinsley, L.P.J., Shelley, J.M.G., 1998. Deposition and element fractionation processes during atmospheric pressure laser sampling for analysis by ICP-MS. Applied Surface Science 127–129, 278–286.

Elhlou, S., Belousova, E., Griffin, W.L., Pearson, N.J., O'Reilly, S.Y., 2006. Trace element and isotopic composition of GJ-red zircon standard by laser ablation. Geochimica et Cosmochimica Acta 70, A158.

Fu, B., Paul, B., Cliff, J., Bröcker, M., Bulle, F., 2012. O–Hf isotope constraints on the origin of zircon in high-pressure mélange blocks and associated matrix rocks from Tinos and Syros, Greece. European Journal of Mineralogy 24, 277–287.

Gao, S., Ling, W.L., Qiu, Y.M., Lian, Z., Hartmann, G., Simon, K., 1999. Contrasting geochemical and Sm–Nd isotopic compositions of Archean metasediments from the Kongling high-grade terrain of the Yangtze Craton: evidence for cratonic evolution and redistribution of REE during crustal anatexis. Geochimica et Cosmochimica Acta 63, 2071–2088.

Gao, S., Yang, J., Zhou, L., Li, M., Hu, Z.C., Guo, J.L., Yuan, H.L., Gong, H.J., Xiao, G.Q., Wei, J.Q., 2011. Age and growth of the Archean Kongling Terrain, South China, with emphasis on 3.3 Ga granitoid gneisses. American Journal of Science 311, 153–182.

Gerdes, A., Zeh, A., 2009. Zircon formation versus zircon alteration – new insights from combined U–Pb and Lu–Hf in-situ LA-ICP-MS analyses, and consequences for the interpretation of Archean zircon from the Central Zone of the Limpopo Belt. Chemical Geology 261, 230–243.

Greentree, M.R., Li, Z.-X., 2008. The oldest known rocks in south-western China: SHRIMP U–Pb magmatic crystallisation age and detrital provenance analysis of the Paleoproterozoic Dahongshan Group. Journal of Asian Earth Sciences 33, 289–302.

Griffin, W.L., Wang, X., Jackson, S.E., Pearson, N.J., O'Reilly, S.Y., Xu, X.S., Zhou, X.M., 2002. Zircon chemistry and magma mixing, SE China: in-situ analysis of Hf isotopes, Tonglu and Pingtan igneous complexes. Lithos 61, 237–269.

Harrison, T.M., Schmitt, A.K., McCulloch, M.T., Lovera, O.M., 2008. Early ($\geq$4.5 Ga) formation of terrestrial crust: Lu–Hf, δ^{18}O, and Ti thermometry results for Hadean zircons. Earth and Planetary Science Letters 268, 476–486.

Hawkesworth, C.J., Kemp, A.I.S., 2006. Using hafnium and oxygen isotopes in zircons to unravel the record of crustal evolution. Chemical Geology 226, 144–162.

Hawkesworth, C.J., Dhuime, B., Pietranik, A.B., Cawood, P.A., Kemp, A.I.S., Storey, C.D., 2010. The generation and evolution of the continental crust. Journal of the Geological Society 167, 229–248.

Hiess, J., Bennett, V.C., Nutman, A.P., Williams, I.S., 2011. Archaean fluid-assisted crustal cannibalism recorded by low δ^{18}O and negative $\varepsilon_{Hf(T)}$ isotopic signatures of West Greenland granite zircon. Contributions to Mineralogy and Petrology 161, 1027–1050.

Hoskin, P.W.O., Black, L.P., 2000. Metamorphic zircon formation by solid-state recrystallization of protolith igneous zircon. Journal of Metamorphic Geology 18, 423–439.

Hu, Z.C., Gao, S., Liu, Y.S., Hu, S.H., Chen, H.H., Yuan, H.L., 2008. Signal enhancement in laser ablation ICP-MS by addition of nitrogen in the central channel gas. Journal of Analytical Atomic Spectrometry 23, 1093–1101.

Hu, Z.C., Liu, Y.S., Gao, S., Liu, W.G., Zhang, W., Tong, X.R., Lin, L., Zong, K.Q., Li, M., Chen, H.H., Zhou, L., Yang, L., 2012. Improved in situ Hf isotope ratio analysis of zircon using newly designed X skimmer cone and jet sample cone in combination with the addition of nitrogen by laser ablation multiple collector ICP-MS. Journal of Analytical Atomic Spectrometry 27, 1391–1399.

Jackson, S.E., Pearson, N.J., Griffin, W.L., Belousova, E.A., 2004. The application of laser ablation-inductively coupled plasma-mass spectrometry to in situ U–Pb zircon geochronology. Chemical Geology 211, 47–69.

Jiao, W.F., Wu, Y.B., Yang, S.H., Peng, M., Wang, J., 2009. The oldest basement rock in the Yangtze Craton revealed by zircon U–Pb age and Hf isotope composition. Science in China Series D: Earth Sciences 52, 1393–1399.

Li, X.-H., Li, W.-X., Li, Z.-X., Lo, C.-H., Wang, J., Ye, M.-F., Yang, Y.-H., 2009a. Amalgamation between the Yangtze and Cathaysia Blocks in South China: constraints from SHRIMP U–Pb zircon ages, geochemistry and Nd–Hf isotopes of the Shuangxiwu volcanic rocks. Precambrian Research 174, 117–128.

Li, X.-H., Liu, Y., Li, Q.-L., Guo, C.-H., Chamberlain, K.R., 2009b. Precise determination of Phanerozoic zircon Pb/Pb age by multicollector SIMS without external standardization. Geochemistry, Geophysics, Geosystems 10, Q04010.

Li, X.-H., Li, W.-X., Li, Q.-L., Wang, X.-C., Liu, Y., Yang, Y.-H., 2010a. Petrogenesis and tectonic significance of the ~850 Ma Gangbian alkaline complex in South China: evidence from in situ zircon U–Pb dating, Hf–O isotopes and whole-rock geochemistry. Lithos 114, 1–15.

Li, X.-H., Long, W.-G., Li, Q.-L., Liu, Y., Zheng, Y.-F., Yang, Y.-H., Chamberlain, K.R., Wan, D.-F., Guo, C.-H., Wang, X.-C., Tao, H., 2010b. Penglai zircon megacrysts: a potential new working reference material for microbeam determination of Hf–O isotopes and U–Pb age. Geostandards and Geoanalytical Research 34, 117–134.

Li, X.-H., Li, Z.-X., He, B., Li, W.-X., Li, Q.-L., Gao, Y., Wang, X.-C., 2012. The Early Permian active continental margin and crustal growth of the Cathaysia Block: in situ U–Pb, Lu–Hf and O isotope analyses of detrital zircons. Chemical Geology 328, 195–207.

Ling, W.L., Gao, S., Cheng, J.P., Jiang, L.S., Yuan, H.L., Hu, Z.C., 2006. Neoproterozoic magmatic events within the Yangtze continental interior and along its northern margin and their tectonic implication: constraint from the ELA-ICPMS U–Pb geochronology of zircons from the Mangling and Hannan complexes. Acta Petrologica Sinica 22, 387–396.

Liu, D.Y., Nutman, A.P., Compston, W., Wu, J.S., Shen, Q.H., 1992. Remnants of $\geq$3800 Ma crust in the Chinese part of the Sino-Korean craton. Geology 20, 339–342.

Liu, Y.S., Hu, Z.C., Gao, S., Günther, D., Xu, J., Gao, C.G., Chen, H.H., 2008a. In situ analysis of major and trace elements of anhydrous minerals by LA-ICP-MS without applying an internal standard. Chemical Geology 257, 34–43.

Liu, Y.S., Zong, K.Q., Kelemen, P.B., Gao, S., 2008b. Geochemistry and magmatic history of eclogites and ultramafic rocks from the Chinese continental scientific drill hole: subduction and ultrahigh-pressure metamorphism of lower crustal cumulates. Chemical Geology 247, 133–153.

Liu, Y.S., Gao, S., Hu, Z.C., Gao, C.G., Zong, K.Q., Wang, D.B., 2010. Continental and oceanic crust recycling-induced melt–peridotite interactions in the Trans-North China Orogen: U–Pb dating, Hf isotopes and trace elements in zircons from mantle xenoliths. Journal of Petrology 51, 537–571.

Liu, Y., Li, X.-H., Li, Q.-L., Tang, G.-Q., Yin, Q.-Z., 2011. Precise U–Pb zircon dating at a scale of <5 micron by the CAMECA 1280 SIMS using a Gaussian illumination probe. Journal of Analytical Atomic Spectrometry 26, 845–851.

Ludwig, K., 2012. User's Manual for Isoplot 3.75: A Geochronological Toolkit for Microsoft Excel. Berkeley Geochronology Center Special Publication No. 5, pp. 1–75.

McDonough, W.F., Sun, S.S., 1995. The composition of the Earth. Chemical Geology 120, 223–253.

Mojzsis, S.J., Harrison, T.M., Pidgeon, R.T., 2001. Oxygen-isotope evidence from ancient zircons for liquid water at the Earth's surface 4,300 Myr ago. Nature 409, 178–181.

Nutman, A.P., McGregor, V.R., Friend, C.R.L., Bennett, V.C., Kinny, P.D., 1996. The Itsaq Gneiss Complex of southern West Greenland: the world's most extensive record of early crustal evolution (3900–3600 Ma). Precambrian Research 78, 1–39.

Nutman, A.P., Bennett, V.C., Friend, C.R.L., McGregor, V.R., 2000. The early Archaean Itsaq Gneiss Complex of southern West Greenland: the importance of field observations in interpreting age and isotopic constraints for early terrestrial evolution. Geochimica et Cosmochimica Acta 64, 3035–3060.

Nutman, A.P., Wan, Y.S., Liu, D.Y., 2009. Integrated field geological and zircon morphology evidence for ca. 3.8 Ga rocks at Anshan: comment on "Zircon U–Pb and Hf isotopic constraints on the Early Archean crustal evolution in Anshan of the North China Craton" by Wu et al. [Precambrian Res. 167 (2008) 339–362]. Precambrian Research 172, 357–360.

Peng, M., Wu, Y.B., Gao, S., Zhang, H.F., Wang, J., Liu, X.C., Gong, H.J., Zhou, L., Hu, Z.C., Liu, Y.S., Yuan, H.L., 2012. Geochemistry, zircon U–Pb age and Hf isotope compositions of Paleoproterozoic aluminous A-type granites from the Kongling terrain, Yangtze Block: constraints on petrogenesis and geologic implications. Gondwana Research 22, 140–151.

Qiu, Y.M., Gao, S., McNaughton, N.J., Groves, D.I., Ling, W.L., 2000. First evidence of >3.2 Ga continental crust in the Yangtze Craton of south China and its implications for Archean crustal evolution and Phanerozoic tectonics. Geology 28, 11–14.

Rudnick, R.L., Shan, G., Ling, W.L., Liu, Y.S., McDonough, W.F., 2004. Petrology and geochemistry of spinel peridotite xenoliths from Hannuoba and Qixia, North China craton. Lithos 77, 609–637.

Siebel, W., Shang, C.K., Thern, E., Danišík, M., Rohrmüller, J., 2012. Zircon response to high-grade metamorphism as revealed by U–Pb and cathodoluminescence studies. International Journal of Earth Sciences 101, 2105–2123.

Sláma, J., Košler, J., Condon, D.J., Crowley, J.L., Gerdes, A., Hanchar, J.M., Horstwood, M.S.A., Morris, G.A., Nasdala, L., Norberg, N., Schaltegger, U., Schoene, B., Tubrett, M.N., Whitehouse, M.J., 2008. Plešovice zircon – a new natural reference material for U–Pb and Hf isotopic microanalysis. Chemical Geology 249, 1–35.

Söderlund, U., Patchett, P.J., Vervoort, J.D., Isachsen, C.E., 2004. The ^{176}Lu decay constant determined by Lu–Hf and U–Pb isotope systematics of Precambrian mafic intrusions. Earth and Planetary Science Letters 219, 311–324.

Souders, A.K., Sylvester, P.J., Myers, J.S., 2013. Mantle and crustal sources of Archean anorthosite: a combined in situ isotopic study of Pb–Pb in plagioclase and Lu–Hf in zircon. Contributions to Mineralogy and Petrology 165, 1–24.

Sun, M., Chen, N., Zhao, G., Wilde, S.A., Ye, K., Guo, J., Chen, Y., Yuan, C., 2008. U–Pb zircon and Sm–Nd isotopic study of the Huangtuling granulite, Dabie-Sulu Belt, China: implication for the Paleoproterozoic tectonic history of the Yangtze Craton. American Journal of Science 308, 469–483.

Taylor, S.R., McLennan, S.M., 1985. The Continental Crust: Its Composition and Evolution. Blackwell Scientific Publication, Palo Alto, CA.

Valley, J.W., Kinny, P.D., Schulze, D.J., Spicuzza, M.J., 1998. Zircon megacrysts from kimberlite: oxygen isotope variability among mantle melts. Contributions to Mineralogy and Petrology 133, 1–11.

Valley, J.W., Lackey, J.S., Cavosie, A.J., Clechenko, C.C., Spicuzza, M.J., Basei, M.A.S., Bindeman, I.N., Ferreira, V.P., Sial, A.N., King, E.M., Peck, W.H., Sinha, A.K., Wei, C.S., 2005. 4.4 billion years of crustal maturation: oxygen isotope ratios of magmatic zircon. Contributions to Mineralogy and Petrology 150, 561–580.

Vervoort, J.D., Patchett, P.J., 1996. Behavior of hafnium and neodymium isotopes in the crust: constraints from Precambrian crustally derived granites. Geochimica et Cosmochimica Acta 60, 3717–3733.

Wang, Z.J., Wang, J., Du, Q.D., Deng, Q., Yang, F., 2013. The evolution of the Central Yangtze Block during early Neoarchean time: evidence from geochronology and geochemistry. Journal of Asian Earth Sciences 77, 31–44.

Wiedenbeck, M., Allé, P., Corfu, F., Griffin, W.L., Meier, M., Oberli, F., Quadt, A.V., Roddick, J.C., Spiegel, W., 1995. Three natural zircon standards for U–Th–Pb, Lu–Hf, trace element and REE analyses. Geostandards Newsletter 19, 1–23.

Wiedenbeck, M., Hanchar, J.M., Peck, W.H., Sylvester, P., Valley, J., Whitehouse, M., Kronz, A., Morishita, Y., Nasdala, L., Fiebig, J., Franchi, I., Girard, J.P., Greenwood, R.C., Hinton, R., Kita, N., Mason, P.R.D., Norman, M., Ogasawara, M., Piccoli, P.M., Rhede, D., Satoh, H., Schulz-Dobrick, B., Skår, O., Spicuzza, M.J., Terada, K., Tindle, A., Togashi, S., Vennemann, T., Xie, Q., Zheng, Y.F., 2004. Further characterisation of the 91500 zircon crystal. Geostandards and Geoanalytical Research 28, 9–39.

Woodhead, J.D., Hergt, J.M., 2005. A preliminary appraisal of seven natural zircon reference materials for in situ Hf isotope determination. Geostandards and Geoanalytical Research 29, 183–195.

Wu, Y.B., Zheng, Y.F., Gao, S., Jiao, W.F., Liu, Y.S., 2008. Zircon U–Pb age and trace element evidence for Paleoproterozoic granulite-facies metamorphism and Archean crustal rocks in the Dabie Orogen. Lithos 101, 308–322.

Wu, Y.B., Gao, S., Gong, H.J., Xiang, H., Jiao, W.F., Yang, S.H., Liu, Y.S., Yuan, H.L., 2009. Zircon U–Pb age, trace element and Hf isotope composition of Kongling terrane in the Yangtze Craton: refining the timing of Palaeoproterozoic high-grade metamorphism. Journal of Metamorphic Geology 27, 461–477.

Wu, Y.B., Gao, S., Zhang, H.F., Zheng, J.P., Liu, X.C., Wang, H., Gong, H.J., Zhou, L., Yuan, H.L., 2012. Geochemistry and zircon U–Pb geochronology of Paleoproterozoic arc related granitoid in the Northwestern Yangtze Block and its geological implications. Precambrian Research 200–203, 26–37.

Zhang, S.-B., Zheng, Y.-F., Wu, Y.-B., Zhao, Z.-F., Gao, S., Wu, F.-Y., 2006a. Zircon isotope evidence for ≥3.5 Ga continental crust in the Yangtze Craton of China. Precambrian Research 146, 16–34.

Zhang, S.-B., Zheng, Y.-F., Wu, Y.-B., Zhao, Z.-F., Gao, S., Wu, F.-Y., 2006b. Zircon U–Pb age and Hf–O isotope evidence for Paleoproterozoic metamorphic event in South China. Precambrian Research 151, 265–288.

Zhang, S.-B., Zheng, Y.-F., Wu, Y.-B., Zhao, Z.-F., Gao, S., Wu, F.-Y., 2006c. Zircon U–Pb age and Hf isotope evidence for 3.8 Ga crustal remnant and episodic reworking of Archean crust in South China. Earth and Planetary Science Letters 252, 56–71.

Zhang, S.-B., Zheng, Y.-F., Zhao, Z.-F., Wu, Y.-B., Yuan, H.L., Wu, F.-Y., 2008. Neoproterozoic anatexis of Archean lithosphere: geochemical evidence from felsic to mafic intrusions at Xiaofeng in the Yangtze Gorge, South China. Precambrian Research 163, 210–238.

Zheng, J.P., Griffin, W.L., O'Reilly, S.Y., Lu, F.X., Wang, C.Y., Zhang, M., 2004. 3.6 Ga lower crust in central China: new evidence on the assembly of the North China craton. Geology 32, 229–232.

Zheng, J.P., Griffin, W.L., O'Reilly, S.Y., Zhang, M., Pearson, N., Pan, Y.M., 2006a. Widespread Archean basement beneath the Yangtze Craton. Geology 34, 417–420.

Zheng, Y.-F., Zhao, Z.-F., Wu, Y.-B., Zhang, S.-B., Liu, X., Wu, F.-Y., 2006b. Zircon U–Pb age, Hf and O isotope constraints on protolith origin of ultrahigh-pressure eclogite and gneiss in the Dabie orogen. Chemical Geology 231, 135–158.

Zhou, Q., Herd, C.D.K., Yin, Q.-Z., Li, X.-H., Wu, F.-Y., Li, Q.-L., Liu, Y., Tang, G.-Q., McCoy, T.J., 2013a. Geochronology of the Martian meteorite Zagami revealed by U–Pb ion probe dating of accessory minerals. Earth and Planetary Science Letters 374, 156–163.

Zhou, Q., Yin, Q.-Z., Young, E.D., Li, X.-H., Wu, F.-Y., Li, Q.-L., Liu, Y., Tang, G.-Q., 2013b. SIMS Pb–Pb and U–Pb age determination of eucrite zircons at <5 μm scale and the first 50 Ma of the thermal history of Vesta. Geochimica et Cosmochimica Acta 110, 152–175.